

000 001 002 003 004 005 A Spectral Characterization of Generalization 006 in GCN: Escaping the Curse of Dimensionality 007 008 009

010 **Anonymous authors**
011 Paper under double-blind review
012
013
014
015
016
017
018
019
020
021
022
023
024
025

ABSTRACT

011 Empirically it is observed that Graph Convolution Networks (GCNs) often
012 generalize better than fully connected neural networks (FCNNs) on graph-
013 structured data. While this observation is often attributed to the ability
014 of GCNs to exploit knowledge about the underlying graph structure, a
015 rigorous theoretical explanation remains limited. In this work, we theoreti-
016 cally prove that one factor for the improved generalization of GCNs arises
017 from the spectral representation of the filters or graph convolutional layers.
018 Specifically, we derive generalization bounds that are independent of the
019 number of parameters and instead scale nearly linearly with the number
020 of graph nodes, offering a compelling explanation for their superior perfor-
021 mance in over-parameterized regimes. Furthermore, in the limit of infinite
022 number of nodes, we prove that under certain regularity conditions on the
023 spectrum, GCNs escape the curse of dimensionality and continue to gener-
024 alize well. We demonstrate our conclusions through numerical experiments.
025

026 1 INTRODUCTION 027

028 Graph convolutional neural networks (GCNs) (Defferrard et al., 2016; Kipf & Welling, 2017;
029 He et al., 2022) have emerged as a powerful tool for learning from graph-structured data,
030 enabling applications in various domains such as social networks (Fan et al., 2019), rec-
031 ommender systems (Wu et al., 2022), and protein design (Strokach et al., 2020). The
032 remarkable success of GCNs is largely attributed to their superior performance on unseen
033 data compared to FCNNs, when the data has an underlying graph structure (Dwivedi et al.,
034 2023). However, despite strong theoretical support for the use of GCNs in terms of their
035 expressive power (Zhang et al., 2025), stability (Gama et al., 2020), and transferability (Ruiz
036 et al., 2020), a rigorous theoretical understanding of conditions that allow for an improved
037 generalization capability compared to FCNNs is largely unexplored in the literature.
038

039 Several existing works (Liao et al., 2020; Tang & Liu, 2023; Wang et al., 2025a) characterizing
040 the generalization of GCNs are built on the classical statistical learning theory frameworks
041 such as VC dimension (Vapnik, 2013), PAC-Bayes (Shawe-Taylor & Williamson, 1997), and
042 Rademacher complexity (Bartlett & Mendelson, 2002). However, these bounds typically
043 scale with the raw parameter count in the network, often resulting in very loose bounds
044 compared to empirical observations. In the context of FCNNs, this has led more recent
045 generalization theory frameworks to explore bounds based on information-theory, algorithmic
046 stability, the so-called “double-descent” phenomenon, and properties of the training loss
047 landscape (Hochreiter & Schmidhuber, 1997; Schaeffer et al., 2024; Hellström et al., 2025).
048 For GCNs, there are very few attempts to apply these more modern techniques. Shi et al.
049 (2024) recently showed that GCNs exhibit a phenomenon where test error first increases
050 and then decreases with the label ratio, but their analysis is limited to simple linear GCNs
051 with one filter tap for community stochastic block models (cSBMs). There lacks a general
052 framework for analyzing the generalization of GCNs beyond the classical approaches.
053

054 GCNs are highly structured models that exploit the underlying graph structure using the
055 graph convolution/message passing/filtering operations that share parameters across nodes,
056 unlike FCNNs. This suggests that the *intrinsic* dimension of the convolutional layers is
057 often significantly lower than more basic notions of model dimension like the raw parameter
058

054 count. This structure is often not exploited in the literature, and here we argue that the
 055 spectral domain of the convolutional filters provides a natural representation for the analysis
 056 of GCN generalization. Specifically, leveraging ideas from classical signal processing, we note
 057 that filters or convolutional layers can be effectively represented in terms of their frequency
 058 response, which lies in a space whose dimension is the number of nodes in the graph rather
 059 than the full parameter space. In practice, we need larger number of parameters to have
 060 better expressive power for GCNs. This shift in the perspective from the parameter space
 061 to the frequency response will be crucial to obtain tighter generalization bounds.

062 **Paper contributions.** In this work, we formally exploit the spectral structure of GCNs
 063 to derive sharper generalization bounds. Specifically,

064 (i). We present a general framework that provides generalization bounds for GCNs on
 065 arbitrary graph structures. Our bounds only require computation of well-known and easy-
 066 to-compute complexity measures, such as covering numbers in the spectral domain.
 067

068 (ii). We provide a generalization bound which scales as $\sqrt{Ln_x/N}$, where L represents
 069 number of layers, n_x represents number of nodes and N is number of data points. Our
 070 bounds are independent of the total number of model parameters. These bounds provide
 071 an explanation for the empirical success of GCNs even when the number of parameters
 072 is comparable to or larger than that of FCNNs. Moreover, these bounds are significantly
 073 tighter than state-of-the-art results.

074 (iii). We extend our analysis to graphons (countably infinite sized-graph). By assuming
 075 mild spectral regularity, the bounds scale as $N^{-1/6}$ and are dimension-free, thus effectively
 076 escaping the curse of dimensionality.

077 (iv). Finally, we corroborate our theoretical insights with numerical simulations.
 078

079 The remainder of the paper is organized as follows. In §2, we formulate the learning problem,
 080 discuss the limitations of existing generalization bounds, and motivate the need for a new
 081 approach. In §3, we present our general generalization bounds for GCNs and then present
 082 its application in various regimes. We validate our theoretical findings through numerical
 083 experiments in §4, and conclude the paper in §5.

084 **Notation.** The Hermitian (transpose-conjugate) of a matrix M is denoted by M^H . The
 085 set $\mathbb{O}(n_x, \mathbb{C})$ denotes all $n_x \times n_x$ unitary (orthonormal) matrices with complex entries. The
 086 operator $\text{diag}(\cdot)$ constructs a diagonal matrix with the given vector as its diagonal elements,
 087 while $\text{diag}^\dagger(\cdot)$ denotes the inverse operation, extracting the diagonal entries into a vector.

088 The abbreviations “w.p.” and “a.s.” stand for “with probability” and “almost surely”,
 089 respectively. A function f is said to be Lipschitz continuous if there exists a constant $L > 0$
 090 such that for all $\mathbf{x}_1, \mathbf{x}_2 \in \mathcal{X}$, we have $\|f(\mathbf{x}_1) - f(\mathbf{x}_2)\| \leq L\|\mathbf{x}_1 - \mathbf{x}_2\|$. Moreover, the function
 091 f is said to be Lipschitz smooth if its gradient is Lipschitz continuous.

092 We write $\beta \leq (\text{or } \geq) \mathcal{O}(\alpha)$ to mean that there exists a constant $C > 0$ such that $\beta \leq (\text{or } \geq)$
 093 $C\alpha$ for all α in the domain of interest. The notation $[A]$ denotes the index set $\{1, 2, \dots, A\}$.
 094 The set \mathbb{R}^∞ represents the set of all countably infinite sequences of real numbers.

095 2 PROBLEM FORMULATION

096 Consider a graph $\mathcal{G} = (\mathcal{V}, \mathcal{E}, A)$, where $\mathcal{V} \subseteq [n_x]$ is the vertex set, $\mathcal{E} \subseteq [n_x] \times [n_x]$ is the edge
 097 set, and $A \in \mathbb{R}^{n_x \times n_x}$ is the adjacency matrix (where $A_{ij} = \mathbb{1}_{\mathcal{E}}((i, j))$). Suppose $\mathbf{x} \in \mathbb{R}^{n_x}$ is
 100 a vector supported on the graph \mathcal{G} , also referred to as a graph signal, where each entry x_i
 101 corresponds to the scalar feature at the i -th node. In this work, we are interested in learning
 102 GCN that map the graph signal \mathbf{x} to target $\mathbf{y} \in \mathbb{R}^{n_y}$, where the tuple (\mathbf{x}, \mathbf{y}) is a random
 103 variable drawn from an unknown joint distribution μ .

104 **Graph Convolutional Neural Networks (GCNs)** are among the first proposed graph
 105 neural network (GNN) architectures (Defferrard et al., 2016; Kipf & Welling, 2017). GCNs
 106 are constructed by a sequence of compositions of graph convolutional layers, non-linearities,
 107 and pooling operations. The graph convolution (or filtering) operation is the key building
 block of GCNs that aggregates features (or messages) from neighboring nodes in a linear

108 fashion. Let $\mathcal{H} \subset \mathbb{R}^\infty$ be the set of graph filter coefficients. At the layer $l \in [L]$, the
 109 convolutional map $\phi_l : \mathcal{H} \times \mathbb{R}^{d_l} \rightarrow \mathbb{R}^{d_l}$ is defined as
 110

$$\phi_l(\mathbf{h}, \mathbf{z}) := \sum_{k \in \mathbb{N}} h_k S_l^k \mathbf{z}, \quad (1)$$

112 where $S_l \in \mathbb{S}^{d_l}$ is called convolutional operator associated with the graph \mathcal{G} at layer l (e.g.,
 113 A or any Laplacian operator such as $\text{diag}(A\mathbf{1}) - A$; see [Defferrard et al. \(2016\)](#); [Kipf &](#)
 114 [Welling \(2017\)](#)) and n_f represents the number of filter taps, i.e., the number of non-zero
 115 coefficients in \mathbf{h} . At each layer $l \in [L]$, we have non-linear activation $\sigma_l : \mathbb{R}^{d_l} \rightarrow \mathbb{R}^{d_l}$, (such
 116 as ReLU, tanh, or sigmoid functions). Finally, we have a pooling or resampling operation
 117 $P_l : \mathbb{R}^{d_{l-1}} \rightarrow \mathbb{R}^{d_l}$ that reduces (or increases) the size of the graph at each layer, gradually
 118 making the final prediction compatible with the target vector. The intermediate output at
 119 layer $l \in [L]$ and channel $c \in [C_l]$ is denoted by $\mathbf{x}_l^c \in \mathbb{R}^{d_l}$ and is computed as
 120

$$\mathbf{x}_l^c = P_l \left(\sigma_l \left(\sum_{g \in [C_{l-1}]} \phi_l(\mathbf{h}_l^{(c,g)}, \mathbf{x}_{l-1}^g) \right) \right). \quad (2)$$

121 The map $\mathbf{x}_0^1 (= \mathbf{x}) \rightarrow \mathbf{x}_L^1 (= \hat{\mathbf{y}})$ is called the GCN and is denoted by $\Phi : \mathcal{H} \times \mathbb{R}^{n_x} \rightarrow \mathbb{R}^{n_y}$,
 122 where the set $\mathcal{H} = \{\mathcal{H}^{C_l \times C_{l-1}}\}_{l \in [L]}$ consists of all the filter coefficients. Convolutional
 123 neural networks (CNNs) ([Denker et al., 1988](#)) are a special case of GCNs, since CNN convolutions
 124 operate on regular grid graphs like images, where pixels are nodes (see [§A.1](#)).
 125

126 **Statistical learning problem.** We consider the learning problem of minimizing the un-
 127 regularized risk with loss function $\ell : \mathbb{R}^{n_y} \times \mathbb{R}^{n_y} \rightarrow \mathbb{R}$, sample space Ω , and measure ν :

$$\mathcal{R}_\nu(\mathbf{H}) := \int_{\omega \in \Omega} \ell(\mathbf{y}(\omega), \Phi(\mathbf{H}(\omega), \mathbf{x}(\omega))) d\nu(\omega). \quad (3)$$

128 The goal is to minimize the risk evaluated on the probability measure μ , referred to as
 129 the population risk, i.e., $\hat{\mathbf{H}}_N \in \arg \min_{\mathbf{H} \in \mathcal{H}} \mathcal{R}_\mu(\mathbf{H})$. However, in practice, complete access
 130 to μ is unavailable. For tractability ([Vapnik, 2013](#)), we relax the optimization problem to
 131 the empirical risk minimization by using finite data points $\{(\mathbf{x}_i, \mathbf{y}_i)\}_{i=1}^N$ drawn from the
 132 distribution μ that forms an empirical distribution μ_N and solve the program:
 133

$$\hat{\mathbf{H}}_N \in \arg \min_{\mathbf{H} \in \mathcal{H}} \left\{ \mathcal{R}_{\mu_N}(\mathbf{H}) = \frac{1}{N} \sum_{i \in [N]} \ell(\mathbf{y}_i, \Phi(\mathbf{H}, \mathbf{x}_i)) \right\}. \quad (\text{ERM})$$

134 There arises a natural question of whether the learned parameters $\hat{\mathbf{H}}_N$ perform well on
 135 unseen data; i.e., $\mathcal{R}_\mu(\hat{\mathbf{H}}_N) \approx \mathcal{R}_{\mu_N}(\hat{\mathbf{H}}_N)$? The discrepancy between the population and
 136 empirical risk is called *Generalization Error or Gap*, $\text{GE} : \mathcal{H} \rightarrow \mathbb{R}^+ \cup \{0\}$ and is defined as
 137

$$\text{GE}(\mathbf{H}) := |\mathcal{R}_\mu(\mathbf{H}) - \mathcal{R}_{\mu_N}(\mathbf{H})|. \quad (4)$$

138 Our aim is to derive non-asymptotic probabilistic upper bounds for the random variable
 139 $\text{GE}(\hat{\mathbf{H}}_N)$ that depend explicitly on n_x , \mathcal{H} , and N .
 140

141 **Existing approaches to generalization theory.** Before delving into the details of our
 142 main results, we first discuss several commonly used approaches to generalization theory
 143 and highlight their limitations in the context of GNNs. Broadly speaking, generalization
 144 bounds can be categorized into the following paradigms:
 145

- 146 • *Classical uniform concentration:* This framework aims to compute the generalization error
 147 in the worst-case scenario, in other words, over the entire parameter space. The treatment
 148 of the data distribution varies as follows:
 - 149 – *VC theory* ([Vapnik & Chervonenkis, 1971](#)): One of the earliest and most classical
 150 approaches, VC theory, provides uniform guarantees over the hypothesis class and all
 151 distributions. However, computing VC dimensions for general neural networks is NP-
 152 HARD ([Kranakis et al., 1995](#)), and the resulting bounds are often vacuous.
 - 153 – *Distribution specific* ([Shalev-Shwartz et al., 2009](#)): In contrast to VC theory, these
 154 approaches tighten the bounds by restricting attention to specific classes of data dis-
 155 tributions that are close to practical settings (e.g., sub-Gaussian). While this leads
 156 to improved generalization estimates, the analysis still relies on uniform concentration
 157 over the entire parameter space.

- *Geometric Analysis* (Hochreiter & Schmidhuber, 1997): These connect the geometric properties of empirical risk landscape near found solutions with generalization capability. However, such connections are not always necessary, and counterexamples exist (Dinh et al., 2017; Mulayoff & Michaeli, 2020).
- *PAC-Bayes Bounds* (McAllester, 1998): These adopt a Bayesian perspective, requiring a prior belief over the parameter space, and a posterior observation once training data is seen. The generalization error is then bounded via the KL-divergence between the prior and the posterior, which is typically intractable to compute for general networks.
- *Rademacher and Gaussian complexity* (Bartlett & Mendelson, 2002): These capture the ability of models to fit noise and act as a proxy for bounding generalization error. However, they are difficult to compute for deep architectures without strong assumptions.
- *Algorithmic stability* (Bousquet & Elisseeff, 2002): These bounds measure the stability of learning algorithms under perturbations to the training data. While potentially tight, the stability of commonly used algorithms such as stochastic gradient descent (SGD), ADAM (Kingma & Ba, 2015) does not always hold true for generic networks (Zhang et al., 2022).
- *Information theory* (Hellström et al., 2025): These bounds infer about the generalization error by quantifying the mutual information between the learned parameters and the training data. While these bounds can be tight, they are often infeasible to compute in deep learning settings due to similar issues as that of PAC-Bayes.

Limitations of prior approaches. Given the trade-offs of the aforementioned approaches, we focus on a classical generalization error bound from Shalev-Shwartz et al. (2009), which is based on uniform concentration over the parameter space under a fixed bounded data distribution μ . We present this result as a corollary (see §A.6 for proof) and then point out the limitations of this setting in the context of single-layered, and single-channeled GCN.

Corollary 1. *Let $L = 1$, $\mathcal{H} \subset \mathbb{B}_{n_f}(B)$, and support of μ be bounded by G . Then w.p. of at least $1 - \delta$ it holds that*

$$\sup_{\mathbf{H} \in \mathcal{H}} \text{GE}(\mathbf{H}) \leq \mathcal{O}\left(GB\sqrt{\frac{n_f \ln(N) \ln(n_f/\delta)}{N}}\right). \quad (5)$$

Discussion. For a single layer GCN, the bound in Equation (5) scales with the total number of trainable filter coefficients, n_f . In the limit when $n_f \rightarrow \infty$, the upper bound grows unboundedly, which is undesirable. This is particularly problematic in over-parameterized regimes. However, it is worth noticing the set of functions that can be represented by this GCN is significantly smaller due to the convolutional structure of the layer (see Equation 1). Specifically, since the graph signals are finite-length vectors, the Fourier transform is band-limited and can be represented by \mathbb{C}^{n_x} (see Oppenheim (1999)).

At the crux of proof techniques for uniform concentration bounds lies the computation of hypothesis class complexity, measured by the covering number (to be defined precisely later), which represents the minimal number of hypotheses required to accurately represent the entire hypothesis class under a specified error tolerance. Since network parameters are directly used to construct the hypothesis class, the covering number scales exponentially with the number of parameters, n_f , leading to the bound in Equation (5). However, Fourier theory provides an equivalence between filter coefficients and their spectral representation. Here, we exploit this structure to represent the hypothesis class in terms of the spectral representation of the filters. This makes the covering numbers scale exponentially with the number of nodes, n_x , rather than parameters, leading to tighter bounds in over-parameterized regimes.

3 MAIN RESULT

In this section, we present upper bounds for generalization error for GCNs. In §3.1, we state and discuss the standing assumptions that are required for our main results to hold. Later, in §3.2, our main theorem for GCNs is presented. Finally, in §3.3 we apply our main theorem in various regimes of interest.

216 3.1 STANDING ASSUMPTIONS
217

218 Here, we introduce standing assumptions, and necessary tools. First, we assume that the
219 unknown data distribution μ belongs to sub-Gaussian family.

220 **Assumption 1.** *The input signal \mathbf{x} is a non-degenerate sub-Gaussian vector with proxy
221 variance σ^2 ; i.e., for any $\mathbf{a} \in \mathbb{S}^{n_x-1}$ and for all $t \geq 0$, we have*

$$222 \mathbb{E}[\exp(t(\mathbf{x} - \mathbb{E}[\mathbf{x}], \mathbf{a}))] \leq \exp(t\sigma^2/2), \text{ and } \mathbb{E}[\|\mathbf{x}\|_2^2] > 0.$$

223 The target signal takes the form $\mathbf{y} = g(\mathbf{x}) + \epsilon$, where $g : \mathbb{R}^{n_x} \rightarrow \mathbb{R}^{n_y}$ is L_g -Lipschitz
224 continuous function, and ϵ is an independent sub-Gaussian vector with proxy variance σ_ϵ^2 .
225 As a result, the joint distribution μ is part of sub-Gaussian family.

226 Sub-Gaussian models encompass a wide range of practical scenarios, including bounded dis-
227 tributions, Gaussian distributions (and their mixtures), beta and Dirichlet families, among
228 others. This assumption is mild and widely adopted in the statistical learning theory lit-
229 erature (Pensia et al., 2018; Cao et al., 2021; Tadipatri et al., 2025). In GCN literature,
230 boundedness of data is often assumed (Liao et al., 2020), making our assumption general.
231

232 Next, we assume certain regularity condition on loss and activation function.

233 **Assumption 2.** *The loss ℓ is convex and ζ smooth w.r.t the second argument. The activa-
234 tion function in each layer is 1-Lipschitz continuous.*

235 The convexity and smoothness condition on loss is a very common assumption in the lit-
236 erature. Lipschitz continuity on activation plays a pivotal role in our theoretical analysis
237 similar to Shalev-Shwartz et al. (2009), as it enables sharp concentration guarantees when
238 the inputs are drawn from sub-Gaussian distributions. Importantly, this assumption is not
239 strictly necessary for concentration: weaker conditions can also yield such bounds, albeit
240 with slower rates (Adamczak & Wolff, 2015). Commonly used activations such as ReLU,
241 sigmoid, tanh, and softmax follow Lipschitz continuity (Gao & Pavel, 2017).

242 **Spectral representation.** Foundational blocks of GCNs are the graph filters and they
243 admit a spectral representation. Since the convolutional operators are symmetric, they can
244 be diagonalized as $S = V\Lambda V^H$. The matrix $\Lambda \in \mathbb{C}^{n_x}$ whose diagonal entries are referred to
245 as graph spectrum. The Graph Fourier Transform (GFT) for any signal $\mathbf{z} \in \mathbb{R}^{n_x}$ is defined
246 as $\mathcal{F}\mathbf{z} := V^H\mathbf{z} = \hat{\mathbf{z}} \in \mathbb{C}^{n_x}$, and similarly the inverse GFT is defined as $\mathcal{F}^\dagger \hat{\mathbf{z}} = \mathbf{z}$. By applying
247 GFT on both the sides of Equation (1) we obtain

$$248 \mathcal{F}\phi(\mathbf{h}; \mathbf{z}) = \sum_{k=1}^{n_f} h_k \Lambda^k V^H \mathbf{z} = \left(\sum_{k=1}^{n_f} h_k \Lambda^k \right) \mathcal{F}\mathbf{z}, \quad (6)$$

251 from which we have the spectral representation of graph filter / spectra as $\tilde{h}(\lambda) =$
252 $\sum_{k=1}^{n_f} h_k \lambda^k$. For future use we denote spectra as

$$254 \mathcal{FH} := \left\{ \sum_{k=1}^{n_f} h_k \text{diag}^\dagger(\Lambda^k) : \forall \{h_k\} \in \mathcal{H} \right\} \subseteq \mathbb{C}^{n_x}, \quad (7)$$

256 and likewise the set \mathcal{FH} denotes the spectra of all layers and channels.

258 Finally, we introduce the notion of covering numbers that will be used in our main results.

259 **Definition 1** (ε -Covering Number (Vershynin, 2018)). *Let \mathcal{A} be a set equipped with a semi-
260 metric d . An ε -net of set \mathcal{A} , denoted by $\mathcal{C}(\mathcal{A}, d, \varepsilon)$, is any set of points $\{h'_k\} \subseteq \mathcal{A}$ such that
261 every point $h \in \mathcal{A}$ lies within distance ε of some h'_k ; i.e.,*

$$262 \mathcal{C}(\mathcal{A}, d, \varepsilon) := \{h'_k\} : \forall h \in \mathcal{A}, \exists h'_k \in \mathcal{A} \text{ such that } d(h, h'_k) \leq \varepsilon.$$

263 The ε -covering number of \mathcal{A} , denoted by $\mathcal{N}(\mathcal{A}, d, \varepsilon)$ is the minimal cardinality of $\mathcal{C}(\mathcal{A}, d, \varepsilon)$.
264 The natural logarithm of covering number is called the metric entropy of the set \mathcal{A} .

266 3.2 A SHARP GENERALIZATION BOUND FOR GCNs
267

268 With the above assumptions and definitions in place, We now present the main general-
269 ization error bound. To avoid notational clutter, we omit few deterministic constants, and
270 proofs which can be found in the §A.4, and §A.5 respectively.

270 **Theorem 1.** Under the Assumptions 1, and 2. Suppose $\{(\mathbf{x}_i, \mathbf{y}_i)\}_{i \in [N]}$ are i.i.d. samples
 271 drawn from the distribution μ and \mathcal{H} be a compact set. Define the quantities
 272

$$273 \quad L_{\mathcal{X}} := \left(\prod_{l \in [L]} C_l \sup_{\mathbf{h} \in \mathcal{H}} \|\mathcal{F}_l \mathbf{h}\|_2 \right), \quad L_{\mathcal{H}} := \left[\mathbb{E} [\|\mathbf{x}\|_2] + \sup_{l \in [L], \mathbf{h} \in \mathcal{H}} \|\mathcal{F}_l \mathbf{h}\|_2 \right]$$

$$274$$

$$275$$

$$276 \quad K := n_y \zeta [(L_{\mathcal{X}}^2 + L_g^2) \sigma^2 + \sigma_e^2], \quad K' := \max \{ 2L_{\mathcal{H}} [\mathcal{L}_{\mathcal{H}} \Delta_{\|\cdot\|_2}(\mathcal{H}) + \Phi(0; 0)], K + 1 \}.$$

$$277$$

278 Fix a $\delta \in (0, 1]$. Then for any global minimizer $\hat{\mathbf{H}}_N$ of (ERM) w.p. of at least $1 - \delta$ we have
 279

$$280 \quad \text{GE}(\hat{\mathbf{H}}_N) \leq \inf_{\varepsilon \in (0, K]} \left(2\varepsilon + K \sqrt{\frac{\ln(3/\delta) + \sum_{l \in [L]} \mathcal{L}_{\mathcal{H}} \ln(\mathcal{N}(\mathcal{F}_l \mathcal{H}, \|\cdot\|_2, \varepsilon/K'))}{2N}} \right) \quad (8)$$

$$281$$

$$282$$

283 **Remarks.** The bound in Equation (16) parallels classical uniform concentration results
 284 for Lipschitz continuous functions under sub-Gaussian data distributions. We now have
 285 flexibility to substitute the covering number of class of spectra considered. The infimum
 286 can be easily upper bounded by certain choices of ε , like demonstrated in §3.3. **Constants**
 287 $\mathcal{L}_{\mathcal{X}}$ (or $\mathcal{L}_{\mathcal{H}}$) are the Lipschitz constants of the GCN w.r.t. the input data (or parameters).
 288 K is the sub-Gaussian proxy variance (or an upper bound thereof) of the GCN's output
 289 and K' is just a internal constant that arises in the proof.

290 **Proof outline.** Our proof technique relies on applying union bound for the tail probabilities
 291 of the empirical process GE, over the hypothesis class \mathcal{H} . This requires computing the
 292 covering number of \mathcal{H} under the metric $d'(\mathbf{h}, \mathbf{h}') := \|\sum_{j \in [n_f]} (h_k - h'_k) S^k\|_2$. However,
 293 by Parseval theorem (Parseval, 1806), we can equivalently compute the metric $d'(\mathbf{h}, \mathbf{h}') =$
 294 $\|\mathcal{F}\mathbf{h} - \mathcal{F}\mathbf{h}'\|_2$. This equivalence is crucial, as it allows us to transfer from \mathbb{R}^{n_f} to \mathbb{C}^{n_x} .
 295

296 **Limitations.** (i) While our results require μ to belong to the sub-Gaussian class. Although
 297 we employ this for technical convenience, the GFT is still applicable. Extensions to heavy-
 298 tailed distributions are possible (Li et al., 2024), albeit with slower error rates.

299 (ii) It is not necessary to solve (ERM) exactly, our results extend to any first-order stationary
 300 points. This requires positive homogeneity of the network $\Phi(\mathbf{H}; \cdot)$ w.r.t its parameters, which
 301 enables connecting the nonconvex and convex programs (Tadipatri et al., 2025).

302 (iii) Finally, our bounds apply only when the convolutional operator S is fixed. For
 303 GNNs that learn S from data, such as Graph Attention Networks (Velivcković et al., 2018;
 304 Franceschi et al., 2019), extending our results is non-trivial, since GFT is not uniform across
 305 draws from μ . Here, prior art often resorts to classical frameworks (Vasileiou et al., 2025).
 306

307 3.3 ESCAPING OVER-PARAMETERIZATION IN GCNs

309 In this section, we apply Theorem 1 to graphs in different regimes. In Corollary 2, we
 310 consider the case when graph is finite sized. In Corollary 3, and 4, we study the case of
 311 infinite sized graphs, or referred to as *graphons* (Ruiz et al., 2020).

312 Optimization algorithms such as SGD, ADAM to solve (ERM) often lead to parameters
 313 that are bounded (Reddy & Vidyasagar, 2023). For GCNs this implies that the spectrum
 314 is bounded, such phenomenon is also observed in Ruiz et al. (2020); Wang et al. (2025b).
 315 We now apply Theorem 1 under this boundedness condition.

316 **Corollary 2.** Let various symbols be as in Theorem 1. If $\mathcal{F}\mathcal{H}$ is bounded by 1, then w.p.
 317 of at least $1 - \delta$ it holds that

$$319 \quad \text{GE}(\hat{\mathbf{H}}_N) \leq K \sqrt{\frac{2\mathcal{L}n_x}{N} \ln \left(1 + \max \left\{ \frac{4K'}{K} \sqrt{\frac{2N}{\mathcal{L}n_x}}, e - 1 \right\} \right)} + K \sqrt{\frac{\ln(3/\delta)}{2N}}. \quad (9)$$

$$320$$

$$321$$

322 **Remarks.** From Equation (9), we conclude that the sample complexity is $N \geq \tilde{\mathcal{O}}(\mathcal{L}n_x)$
 323 and independent of the number of parameter n_f . Meanwhile, FCNNs with same number of

Table 1: Comparison of generalization error bounds for GCN.

Model	Work	Technique	$GE(\hat{\mathbf{H}}_N) \leq \tilde{\mathcal{O}}(\cdot)$
FCNN	Bartlett et al. (2019)	VC-dimension	$\sqrt{((L-1)n_x^2 + n_y n_x)/N}$
GCN	Scarselli et al. (2018)	VC-dimension	$\sqrt{L^2 n_f^4 n_x^2 / N}$
	Liao et al. (2020)	PAC-Bayes ($n_f = 2$)	$\sqrt{L^2 n_x / N}$
	Garg et al. (2020)	Rademacher complexity	$\sqrt{L n_x^3 / N}$
Ours		Covering number	$\sqrt{L n_x / N}$

layers and hidden dimensions would require $N \geq \tilde{\mathcal{O}}((L-1)n_x^2 + n_y n_x)$ (Bartlett et al., 2019). Ours bound provide theoretical evidence for the empirical success of GCNs over FCNNs.

Comparison with state-of-the-art bounds. Our generalization bounds are not only independent of the number of parameters, but also outperform existing state-of-the-art bounds for GCNs (see Table 1). Scarselli et al. (2018) employ VC-theory framework, their analysis yields a sample complexity of $N \geq \tilde{\mathcal{O}}(L^2 n_f^4 n_x^2)$, which scales poorly with L , n_f and n_x . Liao et al. (2020) obtained slightly tighter bound $N \geq \tilde{\mathcal{O}}(L^2 n_x)$ by using PAC-Bayes framework but they consider GCN with second order graph filters (Kipf & Welling, 2017). This bound scales linearly with the L , and also makes it less effective in simple cases when trying to predict low-pass graph signals, which require countably infinite number of filter coefficients (see Oppenheim (1999)). Garg et al. (2020) showed bounds that have no dependence on n_f , and require a sample complexity of $N \geq \tilde{\mathcal{O}}(L n_x^3)$ by using Rademacher complexity. However, cubic dependence on n_x makes it loose compared to our bound. Tang & Liu (2023) provides generalization bounds through algorithmic stability properties of SGD, but lacks explicit dependence on n_f or n_x . Other works (Wang et al., 2025b;c), use the term “generalization bounds” for GCNs in a different context. Their settings consider the closeness of test performance to the best possible in expectation when the graph itself is generated by a fixed manifold, which is different from our setting. In comparison to other works, our bounds do not scale with n_f . To the best of our knowledge, these are the *first theoretical results* that analyze generalization properties in the spectral domain.

Now we extend our results to infinite node regime where the number of nodes $n_x \rightarrow \infty$, these graphs are called *graphons* (Ruiz et al., 2020). Graphons are very relevant to the study of network science (Vizuete et al., 2021), game theory (Parise & Ozdaglar, 2019), and controls (Gao & Caines, 2019b). In this regime, error bounds in Equation 9 quickly become vacuous. The poor scaling is often referred to as “curse of dimensionality”, this term was first coined by Bellman (1954). However, the spectrum of graphons filters are known to exhibit certain regularity conditions (Ruiz et al., 2020). This curse of dimensionality can be avoided by imposing certain regularity conditions on the spectrum such as Lipschitz continuity or low-pass nature. We now apply Theorem 1 when the spectrum is also Lipschitz continuous.

Corollary 3. *Let various symbols be as in Theorem 1 with $C_l = 1$. If the each layer’s hypothesis class $\mathcal{FH} \subseteq \{\{x_i\} : \forall i \in \mathbb{N}, f \in \mathcal{A}; x_i = f(\lambda_i)\}$, where $\mathcal{A} := \{f : \mathbb{C} \rightarrow \mathbb{C} : \forall \lambda, \lambda' \in \mathbb{C}, |f(\lambda) - f(\lambda')| \leq P|\lambda - \lambda'|, \|f\|_\infty \leq 1, f(0) = 0\}$. Then w.p. of at least $1 - \delta$ we have*

$$GE(\hat{\mathbf{H}}_N) \leq \mathcal{O}\left(\left(\frac{L^{1/6} P^{2/3}}{N^{1/6}}\right) + \sqrt{\frac{\ln(3/\delta)}{N}}\right). \quad (10)$$

Remarks. The error rate only scales as $N^{-1/6}$, which is slower than the central limit theorem rate of $N^{-1/2}$. However, the astounding aspect is that the dependence on n_x and n_f vanishes, effectively escaping the curse of dimensionality. Moreover, it has been well studied that Laplacian of graphons tend to have bounded eigenvalues (Gao & Caines, 2019a). Therefore, the spectrum implicitly satisfies the Lipschitz continuity condition.

Nt & Maehara (2019) observed that GCNs naturally learn low-pass filters for certain datasets. This suggests that spectral response is much more regular than just Lipschitz

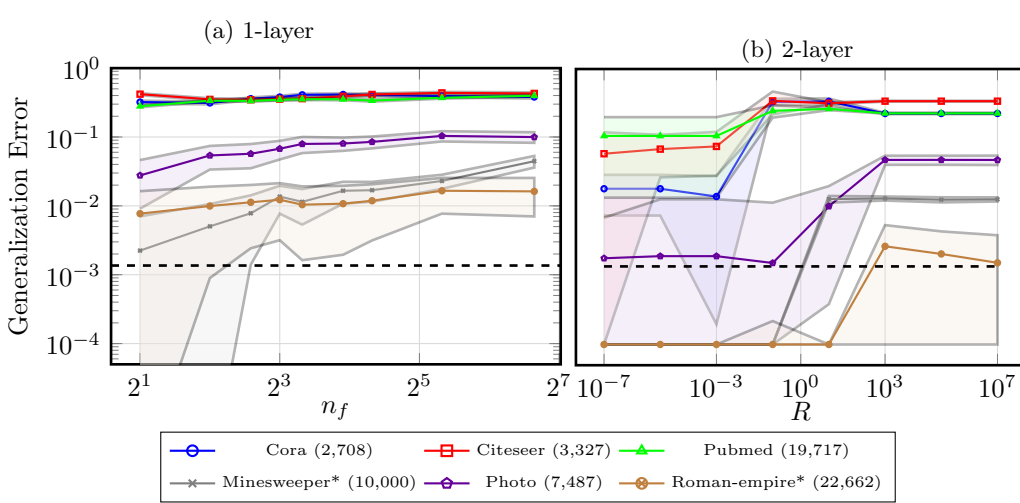


Figure 1: Effect of Lipschitz constant, and filter length on generalization error. Heterophilous datasets are marked with “*”. Dashed line indicates the lowest testing standard error.

continuity. We formalize this regularity and call a spectrum is low-pass with bandwidth γ and order k if the magnitude of the spectra is of form

$$|\tilde{h}(\lambda)| \leq \begin{cases} A_{\text{pass}} & \text{if } |\lambda| \leq \gamma, \\ A_{\text{pass}}/|\lambda|^k & \text{otherwise.} \end{cases} \quad (11)$$

Next, we apply Theorem 1 when the spectrum is also low-pass.

Corollary 4. *Let various symbols be as in Theorem 1 with $L = 1$. If the hypothesis class \mathcal{H} consists of low-pass spectrum with order $k > 1/2$. Then there are deterministic constants $\alpha_k, \beta_k > 0$ such that w.p. of at least $1 - \delta$ we have*

$$\text{GE}(\hat{\mathbf{H}}_N) \leq \alpha_k \sqrt{\frac{\ln(1 + \max\{\beta_k(N/\mathcal{L})^{(2k-1)/4k}, e^{1/(2k-1)^2} - 1\})}{(N/\mathcal{L})^{(2k-1)/2k}}} + K \sqrt{\frac{\ln(3/\delta)}{2N}}. \quad (12)$$

Moreover, in the limit as $k \rightarrow \infty$ the above relation evaluates to

$$\text{GE}(\hat{\mathbf{H}}_N) \leq 8 \sqrt{\frac{\mathcal{L} \ln(1 + A_{\text{pass}} \sqrt{8N/\mathcal{L}})}{2N}} + K \sqrt{\frac{\ln(3/\delta)}{2N}}. \quad (13)$$

Remarks. For k th order low-pass spectrum, the generalization error scales as $N^{-(2k-1)/4k}$, as soon as $k \geq 0.75$ we obtain a faster rate than Corollary 3. In the limit when $k \rightarrow \infty$, we recover the best possible rate of $N^{-1/2}$. This indicates that enforcing low-pass filters is beneficial for generalization. However, it is not necessarily true that such constraints yield better expressive power or training performance.

4 NUMERICAL SIMULATIONS

In this section, we corroborate our insights by performing numerical simulations. First, to validate our theoretical upper bounds with empirical observations we design a synthetic experiment using Erdos-Renyi-Gilbert model. Finally, we consider several real-world datasets both homophilic (node features are similar when targets are similar) and heterophilic (node features are not similar when targets are similar) to perform node classification. The datasets include Cora, CiteSeer, Pubmed (Yang et al., 2016), Photo, Computers (Shchur et al., 2018), Wikics (Mernyei & Cangea, 2020), Minesweeper, Tolokers, Roman-empire, Amazon-ratings, and Questions (Platonov et al., 2023).

In practice, it is computationally inefficient to implement graph filters of the form in Equation (1) directly, especially for large graphs. To address this, we parametrize graph filters

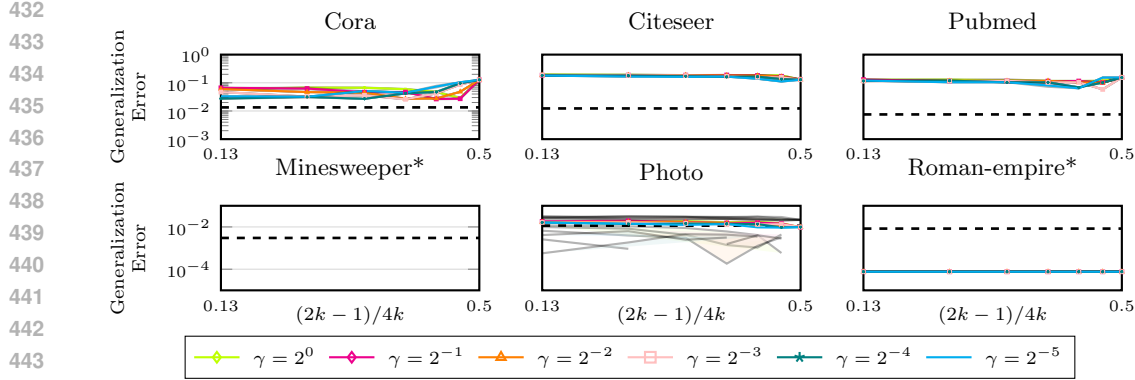


Figure 2: Effect of low-pass spectrum on the generalization error. γ is band-width, and k is exponent of spectrum decay. Heterophilous datasets are marked with “*”. Dashed line indicates the lowest testing standard error.

using a Chebyshev polynomial basis, whose approximation properties are well-studied and known to be min–max optimal and unique in polynomial space (Geddes, 1978).

We adopt the off-the-shelf ChebNet architecture (Defferrard et al., 2016), which is based on Chebyshev polynomials, to implement the GCN layers. Our model uses a multi-layer ChebNet with ReLU activations and is trained using cross-entropy loss. We train for 200 epochs using the ADAM optimizer (Kingma & Ba, 2015) with a learning rate of 0.01. We provide experimental evidence to verify the theoretical bounds from Corollaries 2, 3, and 4. The results are averaged over 5 random seeds. Since the test set itself is random and finite-sampled, we ignore the generalization errors that are less than the standard deviation of the test error fluctuations, i.e., $\ln(n_c)\sqrt{1/2M}$, where n_c is the number of classes, and M is the number of test samples. In our simulations, datasets such as Computers, Wikics, Tolokers, Amazon-ratings, and Questions are not shown because the obtained generalization errors are of order $\approx 10^{-7}$, which is less than the standard deviation of the test error fluctuations, $\approx 10^{-3}$ (see §A.2).

Validation of theoretical bounds. In Figure 3 we plot the empirical and theoretical generalization errors on a synthetic dataset generated using the Erdos-Renyi-Gilbert model for various training sample and sizes. We observe that analyzed upper bounds are consistent with empirical observations. Moreover, the trends of $\mathcal{O}(1/\sqrt{N})$ are consistent with the theoretical bounds. However, there is seems to be a constant gap between the theoretical and empirical errors, which is expected since our bounds are catered to track the trends on the problem parameters but not necessarily tight in constants.

Generalization performance is insensitive to the filter length. Corollary 2 establishes that generalization error is independent of n_f . To verify this claim, we train a 1-layer ChebNet on different datasets while clipping the norm of the parameters to be less than 10^8 for boundedness of the spectrum, with a varying number of filter taps, n_f . Figure 1a shows that the generalization error is relatively constant across large variations in n_f .

Lower Lipschitz constant improves generalization. To verify Corollary 3, we train a 2-layer ChebNet on different datasets via projected ADAM, at each iteration we project the parameters onto a Euclidean ball of desired radius R . This allows us to control the Lipschitz constant of the GCN, since the Lipschitz constant of the filter spectrum is directly proportional to the ℓ_2 norm of the spectrum. In Figure 1b, we vary the R , and observe that lower R (i.e., lower Lipschitz constant) yields better generalization performance consistently across datasets. This empirical evidence supports the upper bound in Equation 10.

Low-pass spectrum yield better generalization. To verify Corollary 4, we train a 1-layer ChebNet composed with a graph low-pass filter having varying bandwidth γ , and order k . Figure 2 shows that the generalization error on a log scale remains invariant to

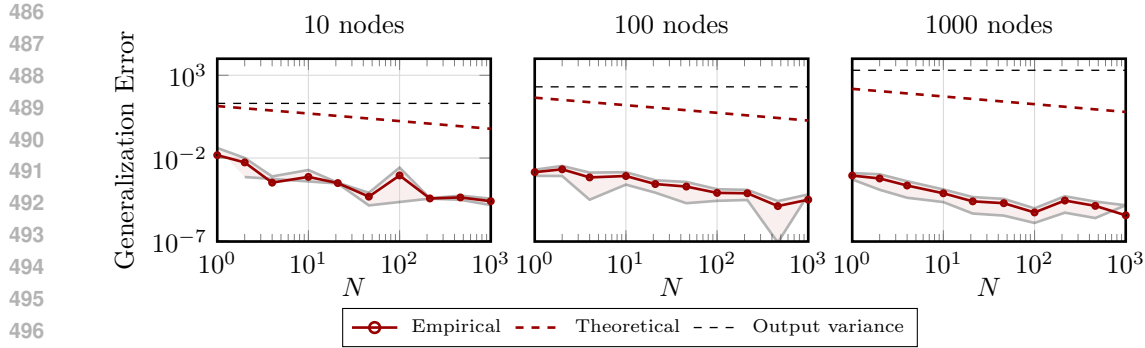


Figure 3: Verification of theoretical upper bounds on Erdos-Rényi-Gilbert model with connection probability 0.05 and node features sampled i.i.d. from $\mathcal{N}(0, 1)$. The scalar targets are generated from a random two-layer ChebNet with unit-norm weights and ReLU activation. Generalization error is computed over N training and 1000 test samples with different graph size.

($2k - 1$)/ $4k$, which is consistent with the exponent in the upper bound of Equation 12. Errors for the Minesweeper dataset is not visible because it is very close to zero.

5 CONCLUSIONS

In this work, we derived sharp generalization bounds for multi-layer, multi-channel GCNs by leveraging classical tools from signal processing and modern techniques in statistical learning theory. Unlike prior approaches that analyze GCNs purely through their parameter space, we adopt a spectral viewpoint of GCN convolutional layers, which admit lower intrinsic dimensionality. By exploiting this spectral structure, we derive generalization bounds that are independent of the total number of trainable parameters, and instead scale nearly linearly with the input dimension or number of nodes. In the finite-node setting, the sample complexity scales nearly linearly with the number of nodes. In the infinite-node setting, under certain mild regularity conditions on the filter spectrum, we show that GCNs provably escape the curse of dimensionality. Our theoretical findings are corroborated by extensive numerical simulations on real-world datasets.

REFERENCES

Radoslaw Adamczak and Paweł Wolff. Concentration inequalities for non-lipschitz functions with bounded derivatives of higher order. *Probability Theory and Related Fields*, 162(3): 531–586, 2015. 5

Peter L Bartlett and Shahar Mendelson. Rademacher and gaussian complexities: Risk bounds and structural results. *Journal of Machine Learning Research*, 3(Nov):463–482, 2002. 1, 4

Peter L Bartlett, Nick Harvey, Christopher Liaw, and Abbas Mehrabian. Nearly-tight vc-dimension and pseudodimension bounds for piecewise linear neural networks. *Journal of Machine Learning Research*, 20(63):1–17, 2019. 7

Richard Bellman. The theory of dynamic programming. *Bulletin of the American Mathematical Society*, 60(6):503–515, 1954. 7

Olivier Bousquet and André Elisseeff. Stability and generalization. *Journal of machine learning research*, 2(Mar):499–526, 2002. 4

Yuan Cao, Quanquan Gu, and Mikhail Belkin. Risk bounds for over-parameterized maximum margin classification on sub-gaussian mixtures. *Advances in Neural Information Processing Systems*, 34:8407–8418, 2021. 5

540 Venkat Chandrasekaran, Benjamin Recht, Pablo A. Parrilo, and Alan S. Willsky. The
 541 Convex Geometry of Linear Inverse Problems. *Foundations of Computational Mathematics*, 12(6):805–849, December 2012. ISSN 1615-3375, 1615-3383. doi: 10.1007/
 542 s10208-012-9135-7. URL <http://link.springer.com/10.1007/s10208-012-9135-7>.
 543 26

544 Michaël Defferrard, Xavier Bresson, and Pierre Vandergheynst. Convolutional neural
 545 networks on graphs with fast localized spectral filtering. *Advances in neural information
 546 processing systems*, 29, 2016. 1, 2, 3, 9

547 548

549 John Denker, W Gardner, Hans Graf, Donnie Henderson, R Howard, W Hubbard,
 550 Lawrence D Jackel, Henry Baird, and Isabelle Guyon. Neural network recognizer for
 551 hand-written zip code digits. *Advances in neural information processing systems*, 1, 1988.
 552 3

553 554 Laurent Dinh, Razvan Pascanu, Samy Bengio, and Yoshua Bengio. Sharp minima can
 555 generalize for deep nets. In *International Conference on Machine Learning*, pp. 1019–
 556 1028. PMLR, 2017. 4

557 558 R. M Dudley. Metric entropy of some classes of sets with differentiable boundaries. *Journal
 559 of Approximation Theory*, 10(3):227–236, March 1974. ISSN 0021-9045. doi: 10.1016/
 560 0021-9045(74)90120-8. URL <https://www.sciencedirect.com/science/article/pii/0021904574901208>. 18

561 562 Vijay Prakash Dwivedi, Chaitanya K Joshi, Anh Tuan Luu, Thomas Laurent, Yoshua Ben-
 563 gio, and Xavier Bresson. Benchmarking graph neural networks. *Journal of Machine
 564 Learning Research*, 24(43):1–48, 2023. 1

565 566 Wenqi Fan, Yao Ma, Qing Li, Yuan He, Eric Zhao, Jiliang Tang, and Dawei Yin. Graph
 567 neural networks for social recommendation. In *The world wide web conference*, pp. 417–
 568 426, 2019. 1

569 570 Luca Franceschi, Mathias Niepert, Massimiliano Pontil, and Xiao He. Learning discrete
 571 structures for graph neural networks. In *International conference on machine learning*,
 572 pp. 1972–1982. PMLR, 2019. 6

573 574 Fernando Gama, Joan Bruna, and Alejandro Ribeiro. Stability properties of graph neural
 575 networks. *IEEE Transactions on Signal Processing*, 68:5680–5695, 2020. doi: 10.1109/TSP.2020.3026980. 1

576 577 Bolin Gao and Lacra Pavel. On the properties of the softmax function with application
 578 in game theory and reinforcement learning. *CoRR*, abs/1704.00805, 2017. URL <http://arxiv.org/abs/1704.00805>. 5

579 580 Shuang Gao and Peter E Caines. Spectral representations of graphons in very large network
 581 systems control. In *2019 IEEE 58th conference on decision and Control (CDC)*, pp.
 582 5068–5075. IEEE, 2019a. 7

583 584 Shuang Gao and Peter E Caines. Graphon control of large-scale networks of linear systems.
 585 *IEEE Transactions on Automatic Control*, 65(10):4090–4105, 2019b. 7

586 587 Vikas Garg, Stefanie Jegelka, and Tommi Jaakkola. Generalization and representational
 588 limits of graph neural networks. In *International conference on machine learning*, pp.
 589 3419–3430. PMLR, 2020. 7

590 591 K. O. Geddes. Near-Minimax Polynomial Approximation in an Elliptical Region. *SIAM
 592 Journal on Numerical Analysis*, 15(6):1225–1233, 1978. doi: 10.1137/0715083. URL
 593 <https://doi.org/10.1137/0715083>. eprint: <https://doi.org/10.1137/0715083>. 9

594 595 Mingguo He, Zhewei Wei, and Ji-Rong Wen. Convolutional neural networks on graphs with
 596 chebyshev approximation, revisited. *Advances in neural information processing systems*,
 597 35:7264–7276, 2022. 1

594 Fredrik Hellström, Giuseppe Durisi, Benjamin Guedj, Maxim Raginsky, et al. Generalization
 595 bounds: Perspectives from information theory and pac-bayes. *Foundations and Trends®*
 596 in Machine Learning

597, 18(1):1–223, 2025. 1, 4

598 Sepp Hochreiter and Jürgen Schmidhuber. Flat minima. *Neural computation*, 9(1):1–42,
 599 1997. 1, 4

600 Wassily Hoeffding. Probability inequalities for sums of bounded random variables. *Journal*
 601 of the American statistical association

602, 58(301):13–30, 1963. 16

603 John J Irwin, Teague Sterling, Michael M Mysinger, Erin S Bolstad, and Ryan G Coleman.
 604 Zinc: a free tool to discover chemistry for biology. *Journal of chemical information and*
 605 *modeling*, 52(7):1757–1768, 2012. 26

606 Diederik P. Kingma and Jimmy Ba. Adam: A method for stochastic optimization. In Yoshua
 607 Bengio and Yann LeCun (eds.), *3rd International Conference on Learning Representations*,
 608 *ICLR 2015, San Diego, CA, USA, May 7-9, 2015, Conference Track Proceedings*,
 609 2015. URL <http://arxiv.org/abs/1412.6980>. 4, 9

610

611 Thomas N Kipf and Max Welling. Semi-supervised classification with graph convolutional
 612 networks. In *International Conference on Learning Representations*, 2017. 1, 2, 3, 7

613 Evangelos Kranakis, Danny Krizanc, Berthold Ruf, Jorge Urrutia, and Gerhard J Woegin-
 614 ger. Vc-dimensions for graphs. In *Graph-Theoretic Concepts in Computer Science: 21st*
 615 *International Workshop, WG'95 Aachen, Germany, June 20–22, 1995 Proceedings* 21,
 616 pp. 1–13. Springer, 1995. 3

617

618 Shaojie Li, Bowei Zhu, and Yong Liu. Algorithmic stability unleashed: Generalization
 619 bounds with unbounded losses. In Ruslan Salakhutdinov, Zico Kolter, Katherine Heller,
 620 Adrian Weller, Nuria Oliver, Jonathan Scarlett, and Felix Berkenkamp (eds.), *Proceedings*
 621 of the 41st International Conference on Machine Learning, volume 235 of *Proceedings of*
 622 *Machine Learning Research*, pp. 29489–29510. PMLR, 21–27 Jul 2024. URL <https:///proceedings.mlr.press/v235/li24cs.html>. 6

623

624 Renjie Liao, Raquel Urtasun, and Richard Zemel. A pac-bayesian approach to generalization
 625 bounds for graph neural networks. In *International Conference on Learning Representa-
 626 tions*, 2020. 1, 5, 7

627

628 David A McAllester. Some pac-bayesian theorems. In *Proceedings of the eleventh annual*
 629 *conference on Computational learning theory*, pp. 230–234, 1998. 4

630 Péter Mernyei and Cuatualina Cangea. Wiki-cs: A wikipedia-based benchmark for graph
 631 neural networks. *arXiv preprint arXiv:2007.02901*, 2020. 8

632

633 Rotem Mulayoff and Tomer Michaeli. Unique properties of flat minima in deep networks.
 634 In *International conference on machine learning*, pp. 7108–7118. PMLR, 2020. 4

635

636 Hoang Nt and Takanori Maehara. Revisiting graph neural networks: All we have is low-pass
 637 filters. *arXiv preprint arXiv:1905.09550*, 2019. 7

638

639 Alan V Oppenheim. *Discrete-time signal processing*. Pearson Education India, 1999. 4, 7

640

641 Francesca Parise and Asuman Ozdaglar. Graphon games. In *Proceedings of the 2019 ACM*
 642 *Conference on Economics and Computation*, pp. 457–458, 2019. 7

643

644 Marc-Antoine Parseval. Mémoire sur les séries et sur l'intégration complète d'une équation
 645 aux différences partielles linéaires du second ordre, à coefficients constants. *Mém. prés.*
 646 *par divers savants, Acad. des Sciences, Paris*,(1), 1(638-648):42, 1806. 6

647

Ankit Pensia, Varun Jog, and Po-Ling Loh. Generalization error bounds for noisy, iterative
 648 algorithms. In *2018 IEEE International Symposium on Information Theory (ISIT)*, pp.
 649 546–550. IEEE, 2018. 5

648 Oleg Platonov, Denis Kuznedelev, Michael Diskin, Artem Babenko, and Liudmila
 649 Prokhorenkova. A critical look at the evaluation of gnns under heterophily: Are we
 650 really making progress? In *The Eleventh International Conference on Learning Repre-*
 651 *sentations*, 2023. 8

652 Tadipatri Uday Kiran Reddy and Mathukumalli Vidyasagar. Convergence of momentum-
 653 based heavy ball method with batch updating and/or approximate gradients. In *2023*
 654 *Ninth Indian Control Conference (ICC)*, pp. 182–187. IEEE, 2023. 6

655 Luana Ruiz, Luiz Chamon, and Alejandro Ribeiro. Graphon neural networks and the trans-
 656 ferability of graph neural networks. *Advances in Neural Information Processing Systems*,
 657 33:1702–1712, 2020. 1, 6, 7

658 Franco Scarselli, Ah Chung Tsoi, and Markus Hagenbuchner. The Vapnik–Chervonenkis
 659 dimension of graph and recursive neural networks. *Neural Networks*, 108:248–259,
 660 December 2018. ISSN 0893-6080. doi: 10.1016/j.neunet.2018.08.010. URL <https://www.sciencedirect.com/science/article/pii/S0893608018302363>. 7

661 Rylan Schaeffer, Zachary Robertson, Akhilan Boopathy, Mikail Khona, Kateryna Pistunova,
 662 Jason William Rocks, Ila R Fiete, Andrey Gromov, and Sanmi Koyejo. Double descent
 663 demystified: Identifying, interpreting & ablating the sources of a deep learning puzzle. In
 664 *The Third Blogpost Track at ICLR 2024*, 2024. 1

665 Shai Shalev-Shwartz, Ohad Shamir, Nathan Srebro, and Karthik Sridharan. Stochastic
 666 convex optimization. In *COLT*, volume 2, pp. 5, 2009. 3, 4, 5, 18, 24

667 John Shawe-Taylor and Robert C Williamson. A pac analysis of a bayesian estimator. In
 668 *Proceedings of the tenth annual conference on Computational learning theory*, pp. 2–9,
 669 1997. 1

670 Oleksandr Shchur, Maximilian Mumme, Aleksandar Bojchevski, and Stephan Günnemann.
 671 Pitfalls of graph neural network evaluation. *arXiv preprint arXiv:1811.05868*, 2018. 8

672 Cheng Shi, Liming Pan, Hong Hu, and Ivan Dokmanić. Homophily modulates double de-
 673 scent generalization in graph convolution networks. *Proceedings of the National Academy
 674 of Sciences*, 121(8):e2309504121, February 2024. doi: 10.1073/pnas.2309504121. URL
 675 <https://www.pnas.org/doi/abs/10.1073/pnas.2309504121>. Publisher: Proceedings
 676 of the National Academy of Sciences. 1

677 Alexey Strokach, David Becerra, Carles Corbi-Verge, Albert Perez-Riba, and Philip M Kim.
 678 Fast and flexible protein design using deep graph neural networks. *Cell systems*, 11(4):
 679 402–411, 2020. 1

680 Uday Kiran Reddy Tadipatri, Benjamin David Haeffele, Joshua Agterberg, and Rene Vi-
 681 dal. A convex relaxation approach to generalization analysis for parallel positively ho-
 682 mogeneous networks. In *The 28th International Conference on Artificial Intelligence and
 683 Statistics*, 2025. URL <https://openreview.net/forum?id=vHdKiqxZNk>. 5, 6, 19

684 Huayi Tang and Yong Liu. Towards understanding generalization of graph neural networks.
 685 In *International Conference on Machine Learning*, 2023. 1, 7

686 Vladimir Vapnik. *The nature of statistical learning theory*. Springer science & business
 687 media, 2013. 1, 3

688 Vladimir Naumovich Vapnik and Aleksei Yakovlevich Chervonenkis. On uniform con-
 689 vergence of the frequencies of events to their probabilities. *Teoriya Veroyatnostei i ee Prime-*
 690 *neniya*, 16(2):264–279, 1971. 3

691 Antonis Vasileiou, Stefanie Jegelka, Ron Levie, and Christopher Morris. Survey on gen-
 692 eralization theory for graph neural networks. *arXiv preprint arXiv:2503.15650*, 2025.
 693 6

702 Petar Veličković, Guillem Cucurull, Arantxa Casanova, Adriana Romero, Pietro Liò, and
 703 Yoshua Bengio. Graph Attention Networks. *International Conference on Learning Rep-*
 704 *resentations*, 2018. URL <https://openreview.net/forum?id=rJXMpikCZ>. 6
 705

706 Roman Vershynin. *High-Dimensional Probability: An Introduction with Applica-*
 707 *tions in Data Science*. Cambridge Series in Statistical and Probabilistic Math-
 708 ematics. Cambridge University Press, Cambridge, 2018. ISBN 978-1-108-41519-
 709 4. doi: 10.1017/9781108231596. URL <https://www.cambridge.org/core/books/highdimensional-probability/797C466DA29743D2C8213493BD2D2102>. 5, 18, 23
 710

711 Renato Vizuete, Federica Garin, and Paolo Frasca. The laplacian spectrum of large graphs
 712 sampled from graphons. *IEEE Transactions on Network Science and Engineering*, 8(2):
 713 1711–1721, 2021. 7

714 Martin J. Wainwright. *High-Dimensional Statistics: A Non-Asymptotic Viewpoint*.
 715 Cambridge Series in Statistical and Probabilistic Mathematics. Cambridge University
 716 Press, Cambridge, 2019. ISBN 978-1-108-49802-9. doi: 10.1017/9781108627771.
 717 URL <https://www.cambridge.org/core/books/highdimensional-statistics/8A91ECEEC38F46DAB53E9FF8757C7A4E>. 25, 27
 718

719 Zhiyang Wang, Juan Cerviño, and Alejandro Ribeiro. Generalization of graph neural net-
 720 works is robust to model mismatch. In *Proceedings of the AAAI Conference on Artificial*
 721 *Intelligence*, volume 39, pp. 21402–21410, 2025a. 1
 722

723 Zhiyang Wang, Juan Cerviño, and Alejandro Ribeiro. Generalization of geometric graph
 724 neural networks with lipschitz loss functions. *IEEE Transactions on Signal Processing*,
 725 2025b. 6, 7

726 Zhiyang Wang, Juan Cerviño, and Alejandro Ribeiro. A manifold perspective on the sta-
 727 tistical generalization of graph neural networks, 2025c. URL <https://openreview.net/forum?id=WRLj18zwz6>. 7
 728

730 Shiwen Wu, Fei Sun, Wentao Zhang, Xu Xie, and Bin Cui. Graph neural networks in
 731 recommender systems: a survey. *ACM Computing Surveys*, 55(5):1–37, 2022. 1
 732

733 Mingqi Yang, Yanming Shen, Rui Li, Heng Qi, Qiang Zhang, and Baocai Yin. A new per-
 734 spective on the effects of spectrum in graph neural networks. In *International Conference*
 735 *on Machine Learning*, pp. 25261–25279. PMLR, 2022. 26

736 Zhilin Yang, William Cohen, and Ruslan Salakhudinov. Revisiting semi-supervised learning
 737 with graph embeddings. In *International conference on machine learning*, pp. 40–48.
 738 PMLR, 2016. 8

739 Bingxu Zhang, Changjun Fan, Shixuan Liu, Kuihua Huang, Xiang Zhao, Jincai Huang, and
 740 Zhong Liu. The expressive power of graph neural networks: A survey. *IEEE Transactions*
 741 *on Knowledge and Data Engineering*, 37(3):1455–1474, 2025. doi: 10.1109/TKDE.2024.
 742 3523700. 1

743 Yikai Zhang, Wenjia Zhang, Sammy Bald, Vamsi Pingali, Chao Chen, and Mayank
 744 Goswami. Stability of sgd: Tightness analysis and improved bounds. In *Uncertainty*
 745 *in artificial intelligence*, pp. 2364–2373. PMLR, 2022. 4
 746

747

748

749

750

751

752

753

754

755

A APPENDIX

In this supplementary material, we discuss the remainder of the proofs for mathematical statements made, extra technical discussion and related work. The below is the table of contents for the appendix.

Contents

1	Introduction	1
2	Problem Formulation	2
3	Main result	4
3.1	Standing Assumptions	5
3.2	A Sharp Generalization Bound for GCNs	5
3.3	Escaping Over-parameterization in GCNs	6
4	Numerical Simulations	8
5	Conclusions	10
A	Appendix	15
		15
A.1	Extensions to CNNs	15
A.2	Extra Numerical Simulations	16
A.3	Existing approach	17
A.4	Constants	18
A.5	Main proofs	18
A.6	Proof of Corollary 1	24
A.7	Proofs of Corollary 2	25
A.8	Proofs of Corollary 6	26
A.9	Proofs of Corollary 3	27
A.10	Proofs of Corollary 4	28

A.1 EXTENSIONS TO CNNs

Example 1. Let $X \in \mathbb{R}^{m \times n}$ be an image. We interpret the graph signal as $\mathbf{x} = \text{vec}(X) \in \mathbb{R}^{m \cdot n}$, where $\text{vec}(\cdot)$ is the vectorization of X obtained by column-wise stacking.

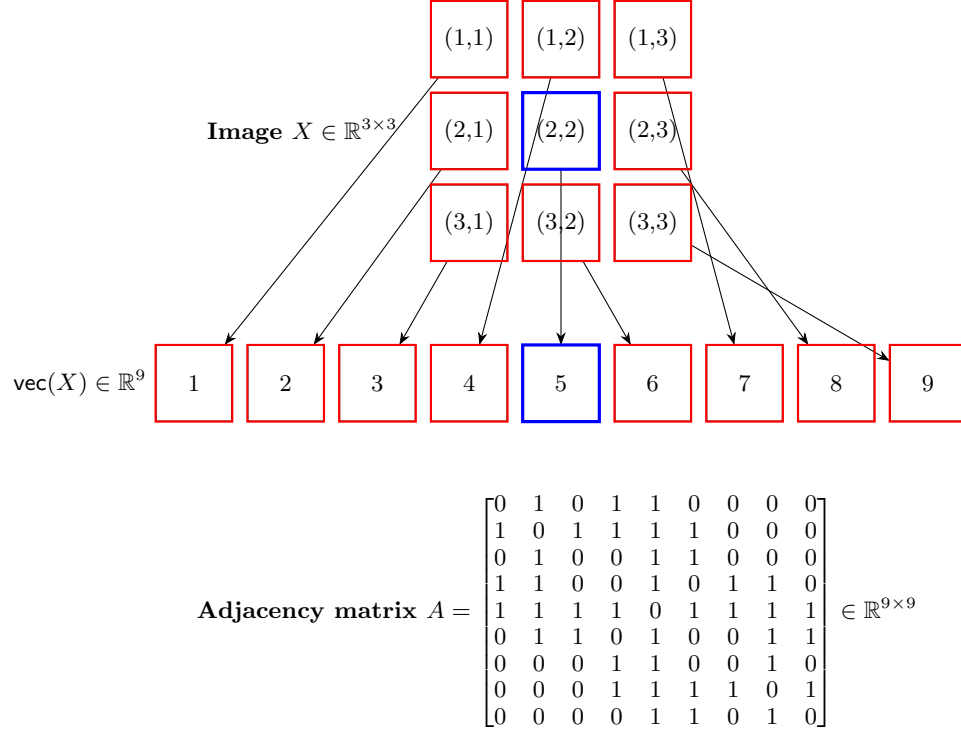
Consider the pixel location $(a, b) \in [m] \times [n]$ the corresponding location in the vectorized image is $a + (b - 1)m$. Suppose that each pixel location (a, b) is connected to its 8-neighbors (if exists) namely $(a - 1, b - 1)$, $(a - 1, b)$, $(a - 1, b + 1)$, $(a, b - 1)$, $(a, b + 1)$, $(a + 1, b - 1)$, $(a + 1, b)$, $(a + 1, b + 1)$. The corresponding locations of these pixels in the vectorized image are

- $(a, b) \rightarrow i := a + (b - 1)m$
- $(a - 1, b - 1) \rightarrow (a - 1) + (b - 2)m = i - (m + 1)$
- $(a - 1, b) \rightarrow (a - 1) + (b - 1)m = i - 1$
- $(a - 1, b + 1) \rightarrow (a - 1) + (b)m = i + (m - 1)$
- $(a, b - 1) \rightarrow a + (b - 2)m = i - m$
- $(a, b + 1) \rightarrow a + (b)m = i + m$
- $(a + 1, b - 1) \rightarrow (a) + (b - 2)m = i - (m - 1)$
- $(a + 1, b) \rightarrow (a) + (b - 1)m = i + 1$
- $(a + 1, b + 1) \rightarrow (a) + (b)m = i + (m + 1).$

810
811 *Effectively the adjacency matrix of the graph is a $m \cdot n \times m \cdot n$ matrix with 8-neighborhood
812 structure. The adjacency matrix A is given by*

813
$$A_{i,j} = \begin{cases} 1, & \text{if } |i - j| \in \{1, m-1, m, m+1\} \\ 0 & \text{otherwise.} \end{cases} \quad (14)$$

814
815 *Pictorial representation of such transformation for 3×3 image is show in Figure 4.*



842 Figure 4: 3×3 image X with symbolic pixel locations (a, b) , its vectorized form $\text{vec}(X)$,
843 and 8-neighborhood (if exists) adjacency matrix A .
844

845 From the above example, we can see that the any image can be represented as a graph signal
846 $\mathbf{x} \in \mathbb{R}^{m \cdot n}$, where m and n are the number of rows and columns of the image respectively.
847 Therefore, our results also apply to CNNs.
848

849 A.2 EXTRA NUMERICAL SIMULATIONS

851 We describe the dataset details in Table 2. We demonstrate both the test error and the
852 generalization error for 2-layer and 10-layer ChebNet in Figure 5. To run our experiments,
853 we use the PyTorch Geometric library for implementing GCNs.

854 In §A.2.1, we discuss the error in estimating the expected risk using empirical test samples.
855

856 A.2.1 EMPIRICAL TEST SAMPLES

858 In practice, we do not have access to the test samples. Therefore, we cannot compute the
859 expected risk to verify the closeness of the empirical risk and the expected risk. Instead, we
860 use a held-out data to estimate the mean. This introduces a small error in the estimation
861 of the expected risk. In the experiments, we consider node classifications tasks with
862 cross-entropy loss, therefore the loss random variables always lies in $[0, \ln(n_c)]$, where n_c is the
863 number of classes. Therefore, we can use Hoeffding's inequality (Hoeffding, 1963) to bound
the error in the estimation of the expected risk.

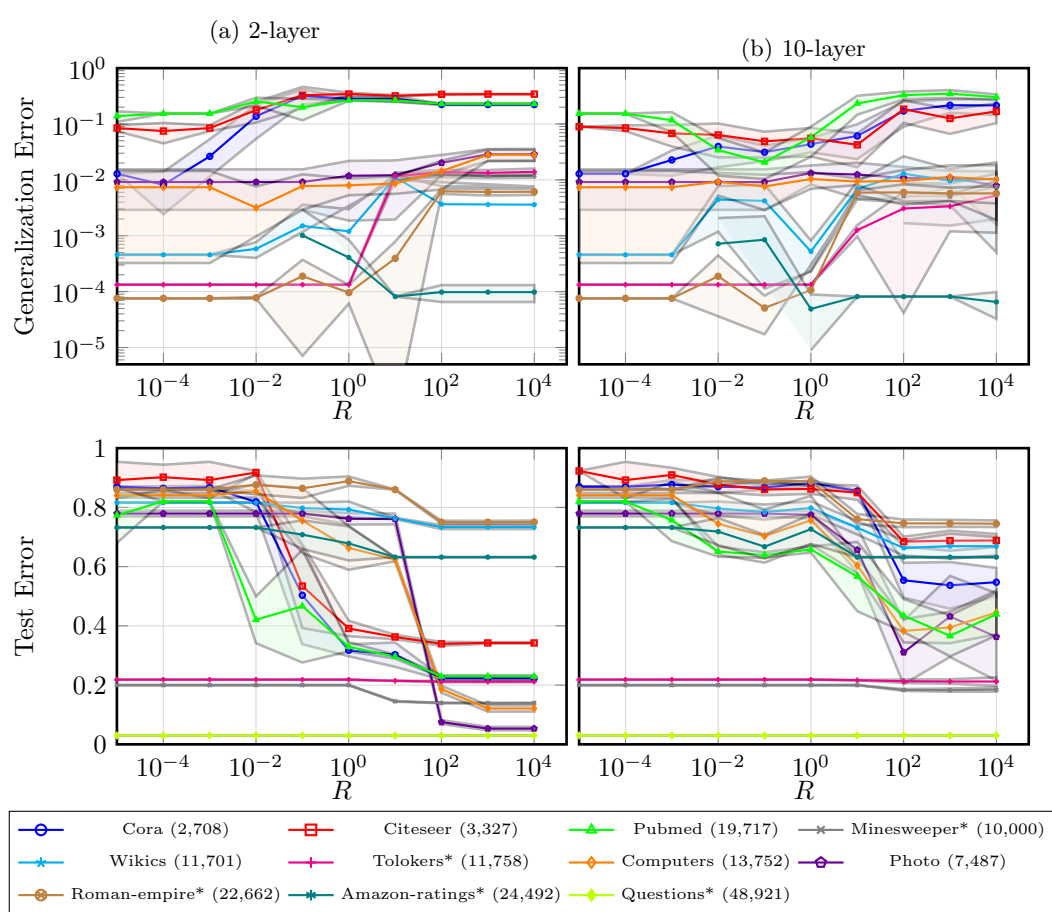


Figure 5: Dataset comparison showing performance across different graph datasets and configurations.

Table 2: Graph datasets used in numerical experiments with their characteristics. $\hat{\beta}$ is the regression coefficient of the linear fit between $\log(\mathbb{P}(\|\mathbf{x} - \mathbb{E}[\mathbf{x}]\|_2 > t))$ and t^2 . Negative $\hat{\beta}$ indicates sub-Gaussian tails.

Dataset	Nodes	Edges	Features	Classes	Homophily	Description	$(\max_i \mathbf{x}_i, \min_i \mathbf{x}_i, \hat{\beta})$	$1 - \mathbb{E}[\ \mathbf{x}\ _0]/n_x$	$1 - \mathcal{E} / \mathcal{V} ^2$
CiteSeer	3,327	9,104	3,703	6	Yes	Citation network	(1.0, 0.0, 0.0)	0.991	0.999
Cora	2,708	10,556	1,433	7	Yes	Citation network	(1.0, 0.0, 0.0)	0.987	0.999
Pubmed	19,717	88,648	500	3	Yes	Citation network	(1.26, 0.0, -7.29)	0.900	0.9997
Amazon-computers	13,752	491,722	767	10	Yes	Product co-purchase network	(1.0, 0.0, 0.0)	0.652	0.994
Amazon-photo	7,487	119,043	765	8	Yes	Product co-purchase network	(1.0, 0.0, 0.0)	0.653	0.996
Amazon-ratings	24,492	93,050	300	5	No	Product rating prediction	(1.87, -1.25, -3.48)	0.000	0.9997
Minesweeper	10,000	39,402	7	2	No	Mine detection in grid	(1.0, 0.0, 0.0)	0.857	0.999
Questions	48,921	153,540	301	2	No	Question classification	(3.36, -1.66, -1.08)	0.152	0.9999
Roman-empire	22,662	32,927	300	18	No	Historical network	(2.08, -1.76, -2.29)	0.003	0.999
Tolokers	11,758	519,000	10	2	No	Worker classification	(1.0, 0.0, -4.39)	0.480	0.992
Wikics	11,701	216,123	300	10	Unknown	Wikipedia CS pages	(2.49, -2.05, -1.74)	0.000	0.997

Proposition 1. Let ℓ be a cross-entropy loss with n_c classes and μ'_M be the empirical distribution of the test set with M samples drawn i.i.d from μ . Suppose that $\hat{\mathbf{H}}_N$ is independent from μ'_M . Fix a $\delta \in (0, 1]$. Then w.p. of at least $1 - \delta$ we have

$$|\mathcal{R}_{\mu'_M}(\hat{\mathbf{H}}_N) - \mathcal{R}_\mu(\hat{\mathbf{H}}_N)| \leq \ln(n_c) \sqrt{\frac{\ln(2/\delta)}{2M}}. \quad (15)$$

A.3 EXISTING APPROACH

Table 1 summarizes existing generalization bounds for GCNs.

918 **Uniform concentration of measure.** The analysis in [Shalev-Shwartz et al. \(2009\)](#) is
 919 typically based on uniform concentration inequalities for Lipschitz continuous functions.
 920 Since the learnt parameters $\hat{\mathbf{H}}_N$ are correlated with the empirical distribution μ_N classical
 921 concentration arguments do not directly apply, that is, closeness of empirical risk to popu-
 922 lation risk. Instead, one must control the deviation uniformly over the parameter space \mathcal{H} ;
 923 i.e., $\text{GE}(\hat{\mathbf{H}}_N) \leq \sup_{\mathbf{H} \in \mathcal{H}} \text{GE}(\mathbf{H})$ a.s. By the monotonicity of probability measures under
 924 inclusion, for any $\varepsilon \in \mathbb{R}$ we have

$$926 \quad \mathbb{P} \left(\text{GE}(\hat{\mathbf{H}}_N) \geq \varepsilon \right) \leq \mathbb{P} \left(\sup_{\mathbf{H} \in \mathcal{H}} \text{GE}(\mathbf{H}) \geq \varepsilon \right)$$

928 To upper bound the right-hand side, one needs a uniform control over the generalization error
 929 across the entire parameter space. A key idea is to relate this to the “size” of the parameter
 930 space, which is captured by the notion of *covering numbers* ([Dudley, 1974](#); [Vershynin, 2018](#)).

931 For instance, suppose the generalization error $\text{GE}(\mathbf{H})$ is K -Lipschitz continuous with respect
 932 to \mathbf{H} under the semi-metric d a.s., that is, for all $\mathbf{H}_1, \mathbf{H}_2 \in \mathcal{H}$: $|\text{GE}(\mathbf{H}_1) - \text{GE}(\mathbf{H}_2)| \leq$
 933 $K \cdot d(\mathbf{H}_1, \mathbf{H}_2)$. Then via few simple algebraic manipulations we can show that

$$935 \quad \mathbb{P} \left(\sup_{\mathbf{H} \in \mathcal{H}} \text{GE}(\mathbf{H}) \geq \varepsilon \right) \leq \mathbb{P} \left(\sup_{\mathbf{H} \in \mathcal{C}(\mathcal{H}, d, \varepsilon)} \text{GE}(\mathbf{H}) \geq (1 + K)\varepsilon \right).$$

937 Since the right-hand side is a union over an ε -net, we can further bound it using the covering
 938 number and for some fixed $\mathbf{H}' \in \mathcal{H}$ independent from μ_N , that is,

$$940 \quad \mathbb{P} \left(\text{GE}(\hat{\mathbf{H}}_N) \geq \varepsilon \right) \leq \mathcal{N}(\mathcal{H}, d, \varepsilon) \cdot \mathbb{P}(\text{for a fixed } \mathbf{H}' \in \mathcal{H} : \text{GE}(\mathbf{H}') \geq (1 + K)\varepsilon).$$

942 The probability term on the right can be upper bounded using standard concentration in-
 943 equalities (e.g., sub-Gaussian). The tightness of the bound depends on the covering number
 944 $\mathcal{N}(\mathcal{H}, d, \varepsilon)$ —smaller values yield tighter generalization bounds.

945 Suppose $\mathcal{H} \subset \mathbb{R}^{n_f}$ (i.e., $L = 1$) then the covering number for $p \geq 1$ we have $\mathcal{N}(\mathcal{H}, \|\cdot\|_p, \varepsilon) \leq$
 946 $\tilde{\mathcal{O}}(1/\varepsilon^{n_f})$, which roughly leads to the bound $\text{GE}(\hat{\mathbf{H}}_N) \propto \sqrt{n_f/N}$. However, in the over-
 947 parameterized regime where $n_f \geq \mathcal{O}(n_x)$, this results in vacuous generalization bounds,
 948 highlighting the need for re-thinking the analysis.

950 A.4 CONSTANTS

952 $\alpha_k = 4 \left(\frac{K}{2(2k-1)} \sqrt{\frac{w_1}{2}} \right)^{(2k-1)/(2k)}$, and $\beta_k = w_2 \left(\frac{2(2k-1)}{K} \sqrt{\frac{2}{w_1}} \right)^{1-1/2k}$, where $w_1 =$
 953 $2 \left(\frac{16A_{\text{pass}}^2}{2k-1} \right)^{1/(2k-1)}$, and $w_2 = 4A_{\text{pass}}K''\sqrt{\zeta(2k)}$, here $\zeta(\cdot)$ is the Riemann zeta function.

956 A.5 MAIN PROOFS

958 In this section, we discuss the proof of Theorem 1, Before which we restate the general
 959 theorem that is applicable to multi-channel GNNs.

961 **Theorem 2.** *Under the Assumptions 1, and 2. Suppose $\{(\mathbf{x}_i, \mathbf{y}_i)\}_{i \in [N]}$ are i.i.d. samples
 962 drawn from the distribution μ and \mathcal{H} be a compact set. Define the quantities*

$$963 \quad L_{\mathcal{X}} := \left(\prod_{l \in [L]} C_l \sup_{\mathbf{h} \in \mathcal{H}} \|\mathcal{F}_l \mathbf{h}\|_2 \right), L_{\mathcal{H}} := \left[\mathbb{E}[\|\mathbf{x}\|_2] + \sup_{l \in [L], \mathbf{h} \in \mathcal{H}} \|\mathcal{F}_l \mathbf{h}\|_2 \right]$$

$$967 \quad K := n_y \zeta \left[(L_{\mathcal{X}}^2 + L_g^2) \sigma^2 + \sigma_e^2 \right], \quad K'' := \max \left\{ 2L_{\mathcal{H}} \left[L_{\mathcal{H}} \Delta_{\|\cdot\|_2}(\mathcal{H}) + \Phi(0; o) \right], K + 1 \right\}.$$

968 Fix a $\delta \in (0, 1]$. Then for any global minimizer $\hat{\mathbf{H}}_N$ of (ERM) w.p. of at least $1 - \delta$ we have

$$970 \quad \text{GE}(\hat{\mathbf{H}}_N) \leq \inf_{\varepsilon \in (0, K]} \left(2\varepsilon + K \sqrt{\frac{\ln(3/\delta) + \sum_{l \in [L]} C_l C_{l-1} \ln(\mathcal{N}(\mathcal{F}_l \mathcal{H}, \|\cdot\|_2, \varepsilon/K''))}{2N}} \right) \quad (16)$$

972 *Proof.* We use Lemma 6 to estimate the Lipschitz constants of the GCN function Φ , denote
 973 the input Lipschitz constant by $L_{\mathcal{X}}$, and the parameter Lipschitz constant by $L_{\mathcal{H}}$. Now by
 974 invoking Lemma 2 with K, K' we obtain

$$975 \mathbb{P} \left(\text{GE}(\hat{\mathbf{H}}_N) > \inf_{\varepsilon \in (0, K]} \left(2\varepsilon + K \sqrt{\frac{\ln(\mathcal{N}(\mathcal{FH}, \sup \|\cdot\|_2, \varepsilon / \max\{K_1, K+1\})) + \ln(3/\delta)}{2N}} \right) \right) \\ 976 \leq \delta.$$

980 By upper bounding $\ln(\mathcal{N}(\mathcal{FH}, \sup \|\cdot\|_2, \varepsilon / \max\{K_1, K+1\}))$ by $\sum_{l \in [L]} C_l C_{l-1} \ln(\mathcal{N}(\mathcal{F}_l \mathcal{H}, \|\cdot\|_2, \varepsilon / \max\{K_1, K+1\}))$ and re-scaling the ε we obtain the desired result. \square

983 First we re-state the uniform concentration of convex functions. In other words, the closeness
 984 of empirical loss and population loss for a given function map.

985 **Lemma 1** (Concentration of Convex loss (Tadipatri et al., 2025)). *Suppose the distribution
 986 μ satisfies the Assumption 1. Consider the estimators from the set of functions $f_\theta : \mathbb{R}^{n_x} \rightarrow
 987 \mathbb{R}^{n_y}$ as parameterized by $\theta \in \Theta$ that are L_Θ -Lipschitz continuous with respective to inputs.
 988 Consider a loss function $\ell : \mathbb{R}^{n_y} \times \mathbb{R}^{n_y} \rightarrow \mathbb{R}$ that is convex and ζ -smooth.*

989 Let $\mathcal{C} \subseteq \mathbb{R}^{n_x}$ be some convex set independent of empirical samples $\{\mathbf{x}_i\}_{i \in [N]}$ that are drawn
 990 i.i.d from μ such that $\mathbb{P}(\forall i \in [N], X_i \in \mathcal{C}) \geq 1 - \delta_C$. Define the quantities

$$992 L^{(\mathcal{C})} := \sup_{\theta, \theta' \in \Theta, \mathbf{z} \in \mathcal{C}} \frac{\|f_\theta(\mathbf{z}) - f_{\theta'}(\mathbf{z})\|}{d(\theta, \theta')}, \quad B^{(\mathcal{C})} := \sup_{\theta \in \Theta, \mathbf{z} \in \mathcal{C}} \|f_\theta(\mathbf{z})\|, \\ 993 994 K := n_Y \zeta \left[(L_\Theta^2 + L_g^2) \sigma_X^2 + \sigma_\epsilon^2 \right], \text{ and} \\ 995$$

$$996 B_{nrm}(\mathcal{C}) := \sup_{\theta, \theta' \in \Theta} \left| \mathbb{E}_{\mathbf{z} \sim \mu} [\|f_{\theta'} \circ \mathcal{P}_{\mathcal{C}}(\mathbf{z}) - f_\theta \circ \mathcal{P}_{\mathcal{C}}(\mathbf{z})\|_2^2] - \mathbb{E}_{\mathbf{z} \sim \mu} [\|f_{\theta'}(\mathbf{z}) - f_\theta(\mathbf{z})\|_2^2] \right| \quad (18)$$

997 where $\mathcal{P}_{\mathcal{C}}(\cdot)$ denotes the Euclidean projection operator onto the set \mathcal{C} . If $L^{(\mathcal{C})}, B^{(\mathcal{C})}, K < \infty$,
 998 and $\hat{\theta}$. Then for any global minimizer of \mathcal{R}_{μ_N} , $\epsilon \in (0, K]$ and some universal constant $c > 0$
 999 we have

$$1000 \mathbb{P} \left(\left| \mathcal{R}_{\mu_N}(\hat{\theta}) - \mathcal{R}_\mu(\hat{\theta}) \right| \geq \epsilon + B_{nrm}(\mathcal{C}) \right) \leq 2\mathcal{N}(\Theta, d, \epsilon / (2L^{(\mathcal{C})}B^{(\mathcal{C})})) \exp \left(-cN(\epsilon/K)^2 \right) \quad (19) \\ 1001 + \delta_C.$$

1004 **Lemma 2.** *Under the settings of Lemma 1, suppose f_0 is constant with value F_0 , and there
 1005 exists positive constants a and b such that $L^{(\mathcal{C})} = a \sup_{\mathbf{z} \in \mathcal{C}} \|\mathbf{z}\| + b$. Define*

$$1007 K_1 := 2\Delta_d(\Theta) (a \|\mathbb{E}[\mathbf{x}]\|_2 + b)^2 + 2F_0 (a \|\mathbb{E}[\mathbf{x}]\|_2 + b).$$

1008 Then there exists a universal positive constant c such that w.p. of at least $1 - \delta$ we have

$$1010 \left| \mathcal{R}_{\mu_N}(\hat{\theta}) - \mathcal{R}_\mu(\hat{\theta}) \right| \leq \inf_{\varepsilon \in (0, K]} \left(2\varepsilon + K \sqrt{\frac{\ln(\mathcal{N}(\Theta, d, \varepsilon / \max\{K_1, 1+K\})) + \ln(3/\delta)}{cN}} \right).$$

1013 *Proof.* The proof involves invoking Lemma 1, and we break it into multiple steps. (I) We will
 1014 choose a convex set \mathcal{C} that contains the data points \mathbf{x} with high probability. (II) Then we
 1015 will bound the key constants such as Lipschitz constant $L^{(\mathcal{C})}$ and $B^{(\mathcal{C})}$. With these constants
 1016 we will move on (III) to controlling the metric entropy, (IV) projection error $B_{nrm}(\mathcal{C})$, and
 1017 (V) existence of data points in \mathcal{C} . Each of the earlier steps induces constraints on the choice
 1018 of \mathcal{C} . In (VI) we will show that a good choice of \mathcal{C} exists that satisfies all the constraints,
 1019 obtaining the final bound.

1020 **(I) Choosing \mathcal{C} :** Set $\mathcal{C} = \mathbb{E}[\mathbf{x}] + \mathbb{B}_2(z)$ for some $z > 0$.

1021 **(II) Bounding key constants:** From our assumption we have

$$1022 L^{(\mathcal{C})} = az + a \|\mathbb{E}[\mathbf{x}]\|_2 + b.$$

1023 To bound the term $B^{(\mathcal{C})}$, on application of the triangle inequality we have

$$1025 B^{(\mathcal{C})} \leq \sup_{\theta \in \Theta, \mathbf{z} \in \mathcal{C}} \|f_\theta(\mathbf{z}) - f_{\theta'}(\mathbf{z})\|_2 + \|f_0(\mathbf{z})\|_2 \leq L^{(\mathcal{C})} \Delta_d(\Theta) + \sup_{\mathbf{z} \in \mathcal{C}} \|f_0(\mathbf{z})\|_2.$$

1026 **(III) Controlling the metric entropy:** Combing the above two inequalities we have
 1027

$$1028 \quad 2L^{(\mathcal{C})}B^{(\mathcal{C})} \leq 2\Delta_d(\Theta) \left[L^{(\mathcal{C})} \right]^2 + 2F_0L^{(\mathcal{C})}. \\ 1029$$

1030 By plugging the choice of \mathcal{C} we have
 1031

$$1032 \quad 2L^{(\mathcal{C})}B^{(\mathcal{C})} \leq 2a^2\Delta_d(\Theta)z^2 + (4a\Delta_d(\Theta) + 2F_0)(a\|\mathbb{E}[\mathbf{x}]\|_2 + b)z \\ 1033 \quad + 2\Delta_d(\Theta)(a\|\mathbb{E}[\mathbf{x}]\|_2 + b)^2 + 2F_0(a\|\mathbb{E}[\mathbf{x}]\|_2 + b), \\ 1034$$

1035 Define $A_1 := 2a^2\Delta_d(\Theta)$, and $B_1 := (4a\Delta_d(\Theta) + 2F_0)(a\|\mathbb{E}[\mathbf{x}]\|_2 + b)$. For some arbitrary
 1036 $\gamma > 0$ and $\alpha \in (0, 1)$ for the relation $\epsilon/2L^{(\mathcal{C})}B^{(\mathcal{C})} \geq \epsilon^{1-\alpha}/\gamma^\alpha$ to hold true, the following
 1037 inequality must hold

$$1038 \quad (\epsilon\gamma)^\alpha \leq A_1z^2 + B_1z + K_1,$$

1039 as $z > 0$, it is necessary and sufficient for z to satisfy
 1040

$$1041 \quad 0 < z \leq z_1(\epsilon, \gamma, \alpha) := \frac{B_1}{2A_1} \left[\sqrt{1 + \frac{(\epsilon\gamma)^\alpha - K_1}{B_1^2}} - 1 \right]. \quad (20) \\ 1042 \\ 1043$$

1044 The admissible ϵ is when $B_1^2 > 4A_1(C_1 - (\epsilon\gamma)^\alpha) \equiv \epsilon > \frac{1}{\gamma}K_1^{1/\alpha}$.
 1045

1046 $z_1(\epsilon, \gamma, \alpha)$ is a continuous function in its arguments, a increasing function of ϵ, γ . In the case
 1047 when $\epsilon\gamma \geq 1$, it is increasing in α and decreasing in α otherwise.

1048 **(IV) Controlling the projection error:** From Corollary 5 we have that

$$1049 \quad B_{nrm}(\mathcal{C}) \leq C_1\sigma^2(a\sigma + a\|\mathbb{E}[\mathbf{x}]\|_2 + b)L_\Theta\Delta_d(\Theta)\exp(-C_2z^2/\sigma^2). \\ 1050$$

1051 Therefore, for $B_{nrm}(\mathcal{C}) \leq \epsilon$ to hold true, it is sufficient for
 1052

$$1053 \quad z \geq z_2(\epsilon, \gamma, \alpha) := \frac{\sigma^2}{C_2} \ln \left(\frac{C_1\sigma^2(a\sigma + a\|\mathbb{E}[\mathbf{x}]\|_2 + b)L_\Theta\Delta_d(\Theta)}{\epsilon} \right). \quad (21) \\ 1054$$

1055 The function z_2 is continuous in its arguments, is strictly decreasing in ϵ , and constant in γ
 1056 and α .

1057 **(V) Probability of existence of \mathbf{x} in \mathcal{C} :** Since \mathbf{x} is sub-Gaussian distribution for some
 1058 universal constant $c > 0$ we have

$$1059 \quad \mathbb{P}(\forall i \in [N], X_i \notin \mathcal{C}) \leq 2\exp(-cNz^2/\sigma^2). \\ 1060$$

1061 Therefore, it is sufficient to choose z such that
 1062

$$1063 \quad \exp(-cNz^2/\sigma^2) \leq \exp \left(\ln \left(\mathcal{N}(\Theta, d, \epsilon/(2L^{(\mathcal{C})}B^{(\mathcal{C})})) \right) - cN(\epsilon/K)^2 \right), \\ 1064$$

1065 when $z \leq z_1$ we have that
 1066

$$1067 \quad \exp(-cNz^2/\sigma^2) \leq \exp \left(\ln \left(\mathcal{N}(\Theta, d, \epsilon/(2L^{(\mathcal{C})}B^{(\mathcal{C})})) \right) - cN(\epsilon/K)^2 \right), \\ 1068 \\ 1069 \leq \exp \left(\ln \left(\mathcal{N}(\Theta, d, \epsilon^{1-\alpha}/\gamma^\alpha) \right) - cN(\epsilon/K)^2 \right).$$

1070 Therefore, we have that
 1071

$$1072 \quad z \geq z_3(\epsilon, \gamma, \alpha, N) := c_3\sigma \sqrt{\max \left\{ \frac{\epsilon^2}{K^2} - \frac{1}{N} \ln \left(\mathcal{N}(\Theta, d, \epsilon^{1-\alpha}/\gamma^\alpha) \right), 0 \right\}}. \quad (22) \\ 1073 \\ 1074$$

1075 The function z_3 is continuous in its arguments, is increasing in ϵ , decreasing in γ , increasing
 1076 in α when $\epsilon\gamma < 1$, and decreasing in α when $\epsilon\gamma > 1$.

1077 **(VI) Existence of good z :** We claim that there exists a good z such that $z_1 \geq z \geq$
 1078 $\max\{z_2, z_3\}$ with a proof presented next. With such a good choice of z we have that

$$1079 \quad \mathbb{P} \left(\left| \mathcal{R}_{\mu_N}(\hat{\theta}) - \mathcal{R}_\mu(\hat{\theta}) \right| \geq 2\epsilon \right) \leq 3\exp \left(\ln \left(\mathcal{N}(\Theta, d, \epsilon^{1-\alpha}/\gamma^\alpha) \right) - cN(\epsilon/K)^2 \right). \quad (23)$$

1080 **Proof of the (VI):** We will consider the equilibrium point of z_2 and z_3 for finite N , and
 1081 in the limit as $N \rightarrow \infty$, that is, we consider the programs
 1082

$$1083 \underline{\epsilon}^{(\gamma, \alpha, N)} := \inf_{\epsilon > 0} \epsilon \text{ s.t. } z_2(\epsilon, \gamma, \alpha) = z_3(\epsilon, \gamma, \alpha, N),$$

$$1085 \epsilon_* := \inf_{\epsilon > 0} \epsilon \text{ s.t. } z_2(\epsilon, \gamma, \alpha) = \lim_{N \rightarrow \infty} z_3(\epsilon, \gamma, \alpha, N) = c_3 \sigma \epsilon / K.$$

1087 Clearly ϵ_* is independent of γ and α , because in the limit the metric entropy term vanishes.
 1088 From the definition of z_3 we have that $z_3(\epsilon, \gamma, \alpha, N) \leq c_3 \sigma \epsilon / K$, and z_2 does not depend on
 1089 N . Therefore, it is true that $\epsilon_* \leq \underline{\epsilon}^{(\gamma, \alpha, N)}$ for any $N > 0$.

1090 Now we find a feasible candidate for γ , consider the program
 1091

$$1092 \gamma_* := \inf_{\gamma > 0} \gamma \text{ s.t. } z_1(\epsilon_*, \gamma, \alpha) \geq z_2(\epsilon_*, \gamma, \alpha) \geq z_3(\epsilon_*, \gamma, \alpha, N).$$

1093 From earlier discussion we know that in terms of γ , z_1 is increasing, z_2 is constant, and z_3
 1094 is decreasing. Moreover, z_1 can grow unboundedly with γ and z_2 is constant. Therefore, γ_*
 1095 certainly exists and is finite. Recall from Equation (23) that for any arbitrary $\beta \geq 0$ and
 1096 $z \in [z_2(\epsilon_*, N^\beta \gamma_*, \alpha), z_1(\epsilon_*, N^\beta \gamma_*, \alpha)]$, we have that
 1097

$$1098 \mathbb{P} \left(\left| \mathcal{R}_{\mu_N}(\hat{\theta}) - \mathcal{R}_\mu(\hat{\theta}) \right| \geq 2\epsilon \right) \leq \exp \left(\ln \left(3 \cdot \mathcal{N}(\Theta, d, \epsilon / (c \gamma_* N^\beta)^\alpha) \right) - cN(\epsilon/K)^2 \right).$$

1100 Now for $\epsilon \in \left[\frac{1}{\gamma_* N^\beta} K_1^{1/\alpha}, K \right]$ and by instantiating Lemma 1 we have that
 1101

$$1103 \mathbb{P} \left(\left| \mathcal{R}_{\mu_N}(\hat{\theta}) - \mathcal{R}_\mu(\hat{\theta}) \right| \geq 2\epsilon \right) \leq \exp \left(\ln \left(3 \cdot \mathcal{N}(\Theta, d, \epsilon / (K \gamma_* N^\beta)^\alpha) \right) - cN(\epsilon/K)^2 \right), \quad (24)$$

1105 the metric entropy was upper bounded due its non-increasing nature in ϵ .

1106 **Failure rate flipping:** Let δ be such that

$$1107 \exp \left(\ln \left(3 \cdot \mathcal{N}(\Theta, d, \epsilon / (K \gamma_* N^\beta)^\alpha) \right) - c'N(\epsilon/K)^2 \right) \leq \delta,$$

1109 by re-arranging the terms we have that
 1110

$$1111 0 \leq K \sqrt{\frac{\ln \left(3 \cdot \mathcal{N}(\Theta, d, \epsilon / (K \gamma_* N^\beta)^\alpha) \right) + \ln(1/\delta)}{cN}} \leq \epsilon.$$

1114 Now we add 2ϵ on both sides to obtain
 1115

$$1116 2\epsilon \leq 2\epsilon + K \sqrt{\frac{\ln \left(3 \cdot \mathcal{N}(\Theta, d, \epsilon / (K \gamma_* N^\beta)^\alpha) \right) + \ln(1/\delta)}{cN}} \leq 3\epsilon. \quad (25)$$

1118 The intermediate term in Equation (25) is a tight estimate in ϵ , using this we obtain
 1119

$$1120 \mathbb{P} \left(\left| \mathcal{R}_{\mu_N}(\hat{\theta}) - \mathcal{R}_\mu(\hat{\theta}) \right| \geq 2\epsilon + K \sqrt{\frac{\ln \left(3 \cdot \mathcal{N}(\Theta, d, \epsilon / (K \gamma_* N^\beta)^\alpha) \right) + \ln(1/\delta)}{cN}} \right) \leq \delta.$$

1122 Since the choices, $\alpha \in (0, 1)$ and $\beta \geq 0$ are arbitrary, we make good choices to obtain the
 1123 tight rates as possible. We have the following cases:

1124 (a) $K + 1 > K_1$: Define
 1125

$$1126 \underline{\beta}(\alpha) := \frac{\ln(1+K)/\alpha - \ln(K\gamma_*)}{\ln(N)},$$

1128 Then we have that $\epsilon / (K \gamma_* N^{\underline{\beta}(\alpha)})^\alpha = \epsilon / (1+K)$. Set $\underline{\alpha} := \max \left\{ \frac{\ln(1+K)}{\ln(K\gamma_*)}, 1 \right\}$, and $\beta = \underline{\beta}(\alpha)$,
 1129

1130 then for any $\alpha \leq \underline{\alpha}$, and $\epsilon \in \left[K \left(\frac{K_1}{1+K} \right)^{1/\alpha}, K \right]$ we have that
 1131

$$1132 \mathbb{P} \left(\left| \mathcal{R}_{\mu_N}(\hat{\theta}) - \mathcal{R}_\mu(\hat{\theta}) \right| \geq 2\epsilon + K \sqrt{\frac{\ln \left(\mathcal{N}(\Theta, d, \epsilon / (1+K)) \right) + \ln(3/\delta)}{cN}} \right) \leq \delta.$$

1134 We choose a sequence $\{\alpha_k\}$ such that $\alpha_k \rightarrow 0$ and bounded away from 0, and $\underline{\alpha}$. Then we
 1135 obtain the bound

$$1137 \mathbb{P} \left(\left| \mathcal{R}_{\mu_N}(\hat{\theta}) - \mathcal{R}_{\mu}(\hat{\theta}) \right| \geq \inf_{\epsilon \in (0, K]} \left(2\epsilon + K \sqrt{\frac{\ln(\mathcal{N}(\Theta, d, \epsilon/(1+K))) + \ln(3/\delta)}{cN}} \right) \right) \leq \delta.$$

1140 (b) $K + 1 < K_1$: Define

$$1141 \overline{\beta}(\alpha) := \frac{2 \ln(K_1)/\alpha - \ln(K\gamma_*)}{\ln(N)},$$

1144 Then we have that for all $\beta = \overline{\beta}(\alpha)$, $\epsilon/(K\gamma_* N^{\overline{\beta}(\alpha)})^\alpha = \epsilon/K_1$. Set $\overline{\alpha} := \max \left\{ \frac{2 \ln(K_1)}{\ln(K\gamma_*)}, 1 \right\}$.

1145 Now we choose a sequence $\{\alpha_k\}$ such that $\alpha_k \rightarrow 0$ and bounded away from 0, and $\overline{\alpha}$. Then
 1146 we obtain the bound

$$1148 \mathbb{P} \left(\left| \mathcal{R}_{\mu_N}(\hat{\theta}) - \mathcal{R}_{\mu}(\hat{\theta}) \right| \geq \inf_{\epsilon \in (0, K]} \left(2\epsilon + K \sqrt{\frac{\ln(\mathcal{N}(\Theta, d, \epsilon/K_1)) + \ln(3/\delta)}{cN}} \right) \right) \leq \delta.$$

1150 This concludes the proof. \square

1152 **Lemma 3.** Suppose $\forall \theta \in \Theta, f_\theta$ is L_Θ -Lipschitz continuous with respect to inputs, and
 1153 $L^{(\mathbb{B}_2(\mathbf{x}))}$ -Lipschitz continuous with respect to parameter for a fixed \mathbf{x} . Then the projection
 1154 difference satisfies the inequality:

$$1156 B_{nrm}(\mathcal{C}) \leq 2L_\Theta \Delta_d(\Theta) \mathbb{E} \left[L^{(\mathcal{C})} + L^{(\mathbb{B}_2(\mathbf{x}))} \right] \mathbb{E} [\|\mathcal{P}_{\mathcal{C}}(\mathbf{x}) - \mathbf{x}\|_2].$$

1158 *Proof.* Recall that the projection difference is defined as

$$\begin{aligned} 1160 B_{nrm}(\mathcal{C}) &= \sup_{\theta, \theta' \in \Theta} \left| \mathbb{E} [\|f_{\theta'} \circ \mathcal{P}_{\mathcal{C}} - f_\theta \circ \mathcal{P}_{\mathcal{C}}\|_2^2 - \|f_{\theta'} - f_\theta\|_2^2] \right| \\ 1161 &= \sup_{\theta, \theta' \in \Theta} \left| \mathbb{E} [\langle f_\theta \circ \mathcal{P}_{\mathcal{C}} - f_\theta - (f_{\theta'} \circ \mathcal{P}_{\mathcal{C}} - f_{\theta'}), f_\theta \circ \mathcal{P}_{\mathcal{C}} - f_{\theta'} \circ \mathcal{P}_{\mathcal{C}} + f_\theta - f_{\theta'} \rangle] \right| \\ 1162 &\leq \sup_{\theta, \theta' \in \Theta} \mathbb{E} [\|f_\theta \circ \mathcal{P}_{\mathcal{C}} - f_\theta - (f_{\theta'} \circ \mathcal{P}_{\mathcal{C}} - f_{\theta'})\|_2] \mathbb{E} [\|f_\theta \circ \mathcal{P}_{\mathcal{C}} - f_{\theta'} \circ \mathcal{P}_{\mathcal{C}} + f_\theta - f_{\theta'}\|_2] \\ 1163 &\leq \sup_{\theta, \theta' \in \Theta} \mathbb{E} [\|f_\theta \circ \mathcal{P}_{\mathcal{C}} - f_\theta\|_2 + \|f_{\theta'} \circ \mathcal{P}_{\mathcal{C}} - f_{\theta'}\|_2] \\ 1164 &\quad \times \mathbb{E} [\|f_\theta \circ \mathcal{P}_{\mathcal{C}} - f_{\theta'} \circ \mathcal{P}_{\mathcal{C}}\|_2 + \|f_\theta - f_{\theta'}\|_2] \\ 1165 &\leq \sup_{\theta, \theta' \in \Theta} 2L_\Theta \mathbb{E} [\|\mathcal{P}_{\mathcal{C}} - I\|_2] \times d(\theta, \theta') \left[\mathbb{E} \left[L^{(\mathcal{C})} + L^{(\mathbb{B}_2(\mathbf{x}))} \right] \right] \\ 1166 &= 2L_\Theta \Delta_d(\Theta) \mathbb{E} \left[L^{(\mathcal{C})} + L^{(\mathbb{B}_2(\mathbf{x}))} \right] \mathbb{E} [\|\mathcal{P}_{\mathcal{C}}(\mathbf{x}) - \mathbf{x}\|_2]. \end{aligned}$$

1173 The second equality is obtained by identity $\|\mathbf{a}\|_\mu^2 - \|\mathbf{b}\|_\mu^2 = \langle \mathbf{a} - \mathbf{b}, \mathbf{a} + \mathbf{b} \rangle_\mu$. Then the third
 1174 inequality follows from the Cauchy-Schwarz inequality. The fourth inequality follows from
 1175 triangular inequality. The fifth inequality follows from the Lipschitz continuity of f with
 1176 respect to inputs and parameters. \square

1177 **Corollary 5.** Under the settings of Lemma 3, if \mathbf{x} is a sub-Gaussian vector with proxy
 1178 variance σ^2 and $L^{(\mathcal{A})} = a \sup_{\mathbf{z} \in \mathcal{A}} \|\mathbf{z}\| + b$ for some $a, b \in \mathbb{R}^+$, then there are universal
 1179 constants $C_1, C_2 > 0$ such that

$$1181 B_{nrm}(\mathbb{E}[\mathbf{x}] + \mathbb{B}_2(z)) \leq C_1 \sigma^2 (\|\mathbb{E}[\mathbf{x}]\| + a\sigma + b) L_\Theta \Delta_d(\Theta) \exp(-C_2 z^2/\sigma^2). \quad (26)$$

1183 *Proof.* From Lemma 3, we have

$$1185 B_{nrm}(\mathcal{C}) \leq 2L_\Theta \Delta_d(\Theta) \mathbb{E} \left[L^{(\mathcal{C})} + L^{(\mathbb{B}_2(\mathbf{x}))} \right] \mathbb{E} [\|\mathcal{P}_{\mathcal{C}}(\mathbf{x}) - \mathbf{x}\|_2].$$

1187 Now since \mathbf{x} is a sub-Gaussian vector with proxy variance σ^2 , we utilize the results from
 1188 Lemma 4 and Lemma ?? to obtain the desired result. \square

1188 **Lemma 4.** Consider the function $f(\mathbf{x}) = a\|\mathbf{x}\| + b$, for some $a, b \in \mathbb{R}^+$. If \mathbf{x} is a sub-
 1189 Gaussian vector with proxy variance σ^2 , there is a universal constant $C_3 > 0$ such that
 1190

$$1191 \quad \mathbb{E}[f(\mathbf{x})] \leq C_3 a \sigma + b. \quad (27)$$

1192 *Proof.* By linearity of expectation, we have
 1193

$$1194 \quad \mathbb{E}[f(\mathbf{x})] = a\mathbb{E}[\|\mathbf{x}\|] + b.$$

1195 For any sub-Gaussian vector \mathbf{x} with proxy variance σ^2 (see [Vershynin \(2018\)](#)), we have
 1196

$$1197 \quad \mathbb{E}[\|\mathbf{x}\|] \leq C_3 \sigma, \quad (28)$$

1198 where C_3 is a universal constant. Substituting this into the expectation obtains our desired
 1199 result. \square
 1200

1201 **Lemma 5.** If \mathbf{x} is a sub-Gaussian vector with proxy variance σ^2 , then for any $z > 0$ there
 1202 are universal constants $C_1, C_2 > 0$ such that

$$1203 \quad \mathbb{E}[\|\mathbf{x} - \mathcal{P}_{\mathbb{E}[\mathbf{x}] + \mathbb{B}_2(z)}(\mathbf{x})\|_2^2] \leq C_1 \sigma^2 \exp(-C_2 z^2 / \sigma^2). \quad (29)$$

1205 *Proof.* By the definition of the projection operator, we have
 1206

$$1207 \quad \mathbf{x} - \mathcal{P}_{\mathbb{E}[\mathbf{x}] + \mathbb{B}_2(z)}(\mathbf{x}) = \left[1 - \frac{z}{\|\mathbf{x} - \mathbb{E}[\mathbf{x}]\|_2} \right]_+ (\mathbf{x} - \mathbb{E}[\mathbf{x}]).$$

1209 Taking the expectation of the squared norm, we have
 1210

$$1211 \quad \mathbb{E}[\|\mathbf{x} - \mathcal{P}_{\mathbb{E}[\mathbf{x}] + \mathbb{B}_2(z)}(\mathbf{x})\|_2^2] = \mathbb{E} \left[\left[1 - \frac{z}{\|\mathbf{x} - \mathbb{E}[\mathbf{x}]\|_2} \right]_+^2 \|\mathbf{x} - \mathbb{E}[\mathbf{x}]\|_2^2 \right].$$

1214 By the homogeneity of ReLU, we can factor out the squared norm to get
 1215

$$1216 \quad \begin{aligned} \mathbb{E}[\|\mathbf{x} - \mathcal{P}_{\mathbb{E}[\mathbf{x}] + \mathbb{B}_2(z)}(\mathbf{x})\|_2^2] &= \mathbb{E}[\|\mathbf{x} - \mathbb{E}[\mathbf{x}]\|_2^2 - z]_+^2, \\ 1217 &= \int_0^\infty \mathbb{P}([\|\mathbf{x} - \mathbb{E}[\mathbf{x}]\|_2^2 - z]_+^2 > k) dk \\ 1218 &= \int_0^\infty \mathbb{P}([\|\mathbf{x} - \mathbb{E}[\mathbf{x}]\|_2^2 - z]_+ > \sqrt{k}) dk \\ 1219 &= \int_0^\infty \mathbb{P}(\|\mathbf{x} - \mathbb{E}[\mathbf{x}]\|_2 > z + \sqrt{k}) dk. \end{aligned}$$

1224 For some universal constants $c'_1, c'_2 > 0$ we have that
 1225

$$1226 \quad \mathbb{E}[\|\mathbf{x} - \mathcal{P}_{\mathbb{E}[\mathbf{x}] + \mathbb{B}_2(z)}(\mathbf{x})\|_2^2] \leq c'_1 \int_0^\infty \exp(-c_2(z + \sqrt{k})^2 / \sigma^2) dk.$$

1228 Set $u = z + \sqrt{k}$, then we have $dk = 2(u - z)du$. Substituting this into the integral gives us
 1229

$$1230 \quad \begin{aligned} \mathbb{E}[\|\mathbf{x} - \mathcal{P}_{\mathbb{E}[\mathbf{x}] + \mathbb{B}_2(z)}(\mathbf{x})\|_2^2] &\leq 2c'_1 \int_z^\infty (u - z) \exp(-c_2 u^2 / \sigma^2) du, \\ 1231 &= 2c'_1 \int_z^\infty u \exp(-c_2 u^2 / \sigma^2) du - 2c'_1 z \int_z^\infty \exp(-c_2 u^2 / \sigma^2) du. \end{aligned}$$

1235 For the first term, we can use the substitution $v = c'_2 u^2 / \sigma^2$, which gives us $(\sigma^2 / c'_2)dv = 2udu$.
 1236 Observe that second term is negative, so we can upper-bound it by 0. Thus, we have
 1237

$$1238 \quad \mathbb{E}[\|\mathbf{x} - \mathcal{P}_{\mathbb{E}[\mathbf{x}] + \mathbb{B}_2(z)}(\mathbf{x})\|_2^2] \leq \frac{\sigma^2 c'_1}{c'_2} \int_{c'_2 z^2 / \sigma^2}^\infty \exp(-v) dv = \frac{c'_1}{c'_2} \sigma^2 \exp(-c'_2 z^2 / \sigma^2).$$

1240 By setting $C_1 = c'_1 / c'_2$ and $C_2 = c'_2$, we obtain the desired result. \square
 1241

Lemma 6. Under the assumption [2](#), the map Φ satisfies the following statements:

1242 1. For any $\mathbf{H} \in \mathcal{H}$, and $\mathbf{x}, \mathbf{x}' \in \mathbb{R}^{n_x}$ we have that

$$1244 1245 1246 \|\Phi(\mathbf{H}, \mathbf{x}) - \Phi(\mathbf{H}, \mathbf{x}')\|_2 \leq \left(\prod_{l \in [L]} C_l \right) \left[\sup_{\mathbf{h} \in \mathcal{H}} \|\mathcal{F}_l \mathbf{h}\|_2 \right] \|\mathbf{x} - \mathbf{x}'\|_2.$$

1247 2. For any $\mathbf{x} \in \mathcal{C}$ and $\mathbf{H}, \mathbf{H}' \in \mathcal{H}$, and some positive constants c_1, c_2 dependent on $\{C_l\}$ we
1248 have

$$1249 1250 1251 1252 1253 1254 \|\Phi(\mathbf{H}, \mathbf{x}) - \Phi(\mathbf{H}', \mathbf{x})\|_2 \leq \left[c_1 \sup_{\mathbf{x} \in \mathcal{C}} \|\mathbf{x}\| + c_2 \sup_{l \in [L], \mathbf{h} \in \mathcal{H}} \|\mathcal{F}_l \mathbf{h}\|_2 \right] \\ \times \left[\sup_{l \in [L], c \in [C_l], g \in [C_{l-1}]} \|\mathcal{F}_l \mathbf{h}_l^{(c,g)} - \mathcal{F}_l \mathbf{h}'_l^{(c,g)}\|_2 \right].$$

1255 1256 *Proof.* Statement 1 is straight forward, each layer and channel has a input Lipschitz constant
1257 $\|\sum_k h_{k,l,c,g} S_l^k\|_2 = \|\mathcal{F}_l \mathbf{h}_l^{(c,g)}\|_2$. Therefore, the effective is just layer-wise product of the
1258 Lipschitz constants, and using the inequality $\|\mathbf{z}\|_2 \leq \sqrt{d} \|\mathbf{z}\|_\infty$, when $\mathbf{z} \in \mathbb{R}^d$.

1259 1260 • For Statement 2 it is cumbersome, but a useful trick is the identity

$$1261 1262 \|\phi_l(\mathbf{h}, \mathbf{x}) - \phi_l(\mathbf{h}', \mathbf{x}')\|_2 \leq [\|\mathbf{x}\|_2 + \|\mathcal{F}_l \mathbf{h}'\|_2] \max\{\|\mathcal{F}_l \mathbf{h} - \mathcal{F}_l \mathbf{h}'\|_2, \|\mathbf{x} - \mathbf{x}'\|_2\}.$$

1263 1264 • For c channel at layer l , we have

$$1265 1266 1267 \|\mathbf{x}_l^c - \mathbf{x}'_l^c\|_2 \leq \sum_{g \in [C_{l-1}]} \left[\|\mathbf{x}_{l-1}^g\|_2 + \|\mathcal{F}_l \mathbf{h}'_l^{(c,g)}\|_2 \right] \max\{\|\mathcal{F}_l \mathbf{h}_l^{(c,g)} - \mathcal{F}_l \mathbf{h}'_l^{(c,g)}\|_2, \|\mathbf{x}_{l-1}^g - \mathbf{x}'_{l-1}^g\|_2\}.$$

1268 1269 • At layer l for some positive constants K_1, K_2 we have

$$1270 1271 1272 1273 1274 1275 1276 \left\| \begin{bmatrix} \mathbf{x}_l^1 \\ \vdots \\ \mathbf{x}_l^{C_l} \end{bmatrix} - \begin{bmatrix} \mathbf{x}'_l^1 \\ \vdots \\ \mathbf{x}'_l^{C_l} \end{bmatrix} \right\|_2 \leq K_1 \left[\left\| \begin{bmatrix} \mathbf{x}_{l-1}^1 \\ \vdots \\ \mathbf{x}_{l-1}^{C_{l-1}} \end{bmatrix} \right\|_2 + K_2 \sup \|\mathcal{F}_l \mathbf{h}'_l^{(c,g)}\|_2 \right] \\ \max \left\{ \sup_{c \in [C_l], g \in [C_{l-1}]} \|\mathcal{F}_l \mathbf{h}_l^{(c,g)} - \mathcal{F}_l \mathbf{h}'_l^{(c,g)}\|_2, \left\| \begin{bmatrix} \mathbf{x}_l^1 \\ \vdots \\ \mathbf{x}_l^{C_{l-1}} \end{bmatrix} - \begin{bmatrix} \mathbf{x}'_l^1 \\ \vdots \\ \mathbf{x}'_l^{C_{l-1}} \end{bmatrix} \right\|_2 \right\}$$

1277 1278 • We recursively apply this inequality for all layers.

□

A.6 PROOF OF COROLLARY 1

1283 First we state a classical theorem from [Shalev-Shwartz et al. \(2009\)](#) with our notation that
1284 we will use in the proof.

1285 **Theorem 3** (Theorem 5 ([Shalev-Shwartz et al., 2009](#))). *Let $\mathcal{H} \subset \mathbb{R}^d$ be bounded by R and
1286 let $\Phi(\mathbf{H}, \mathbf{z})$ be G -Lipschitz continuous with respect to \mathbf{H} for any \mathbf{z} . Then with probability at
1287 least $1 - \delta$ over a sample of size N , for all $\mathbf{H} \in \Theta$ we have:*

$$1288 1289 1290 1291 \text{GE}(\mathbf{H}) \leq \mathcal{O} \left(GB \sqrt{\frac{d \ln(N) \ln(d/\delta)}{N}} \right) \quad (30)$$

1292 **Proof of Corollary 1.** For single-layer, single-channel GCN under the Assumption 2, we
1293 have that $\Phi(\mathbf{H}, \mathbf{x})$ is $\|\mathbf{x}\|_2$ -Lipschitz continuous with respect to \mathbf{H} . From the boundedness
1294 assumption of the data, we have that $\Phi(\mathcal{H}, \mathbf{x})$ is G -Lipschitz continuous with \mathbf{H} for all inputs
1295 \mathbf{x} . Finally since all the filter coefficients are bounded, i.e, $\mathcal{H} \subset \mathbb{R}^{n_f}$ we can instantiate
Theorem 3. This concludes our proof.

1296 A.7 PROOFS OF COROLLARY 2
1297

1298 In this section, we provide the proof of Corollary 2. The proof relies on substituting the
1299 metric entropy of bounded spectral filters into Theorem 1 and computing the infimum.
1300 First we provide classical results on the metric entropy of finite-dimensional spaces which
1301 Corollary 2 and 6 are based on.

1302 **Lemma 7** (Volume ratios and metric entropy Wainwright (2019)). *Consider a pair of norms*
1303 $\|\cdot\|$ *and* $\|\cdot\|'$ *on* \mathbb{R}^d , *and let* \mathbb{B} *and* \mathbb{B}' *be the unit balls (i.e.,* $\mathbb{B} := \{\theta \in \mathbb{R}^d \mid \|\theta\| \leq 1\}$, *with*
1304 \mathbb{B}' *similarly defined). Then the* ε *-covering number of* \mathbb{B} *in the norm* $\|\cdot\|'$ *obeys the bounds*

$$1305 \left(\frac{1}{\varepsilon}\right)^d \frac{\text{vol}(\mathbb{B})}{\text{vol}(\mathbb{B}')} \leq \mathcal{N}(\mathbb{B}, \|\cdot\|', \varepsilon) \leq \left(1 + \frac{2}{\varepsilon}\right)^d \frac{\text{vol}(\mathbb{B})}{\text{vol}(\mathbb{B}')}. \quad (31)$$

1306 As a special case, if $\|\cdot\|$ and $\|\cdot\|'$ are the same norm, then the metric entropy satisfies the
1307 bound

$$1308 d \ln(1/\varepsilon) \leq \ln(\mathcal{N}(\mathbb{B}, \|\cdot\|, \varepsilon)) \leq d \ln(1 + 2/\varepsilon). \quad (32)$$

1309 Lemma 7 gives us a way to compute the metric entropy for the scenario in Corollary 2.
1310 Next, we introduce an auxiliary proposition that helps us compute the inf in Theorem 1.

1311 **Proposition 2.** *Suppose $a > 0$ then the following holds true:*

$$1312 \inf_{x>0} \left(x + a\sqrt{\ln(1+1/x)} \right) < 2a \cdot \max\{1, \sqrt{\ln(1+1/a)}\} \quad (33)$$

1313 *Proof.* Define $f(x, a) := \left(x + a\sqrt{\ln(1+1/x)} \right)$, clearly by the definition of infimum we have
1314 $\inf_{x>0} f(x, a) < f(x, a)$. Choose $x = a$, then we have

$$1315 \inf_{x>0} f(x, a) < a \left(1 + \sqrt{\ln(1+1/a)} \right), \quad (34)$$

1316 when $a \geq 1/(e-1)$ we have $\ln(1+1/a) \leq 1$, therefore we can upper bound $\inf_x f(x, a) < 2a$.
1317 When $a < 1/(e-1)$ we have $\ln(1+1/a) > 1$, therefore we can upper bound

$$1318 \inf_x f(x, a) < a\sqrt{\ln(1+1/a)} + a\sqrt{\ln(1+1/a)\sqrt{\ln(1+1/a)}} \leq 2a\sqrt{\ln(1+1/a)}. \quad (35)$$

1319 This concludes the proof. \square

1320 **Proof of Corollary 2.** We instantiate Theorem 1 $C_l = 1$, with metric entropy from Lemma
1321 7, we have

$$1322 \mathbb{P} \left(\text{GE}(\hat{\mathbf{H}}_N) > \inf_{\varepsilon \in (0, K]} \left\{ 2\varepsilon + K \sqrt{\frac{Ln_x \ln(1 + 2 \max\{K', K+1\}/\varepsilon) + \ln(3/\delta)}{2N}} \right\} \right) \leq \delta.$$

1323 Define $K'' = \max\{K', K+1\}$. Now re-scale $\varepsilon = 2K''\varepsilon'$ this gives us

$$1324 \mathbb{P} \left(\text{GE}(\hat{\mathbf{H}}_N) > \inf_{\varepsilon' \in (0, K/2K'']} \left\{ 4K''\varepsilon' + K \sqrt{\frac{Ln_x \ln(1 + 1/\varepsilon') + \ln(3/\delta)}{2N}} \right\} \right) \leq \delta.$$

1325 We take $4K''$ as common to have

$$1326 \mathbb{P} \left(\text{GE}(\hat{\mathbf{H}}_N) > 4K'' \cdot \inf_{\varepsilon' \in (0, K/2K'']} \left\{ \varepsilon' + \frac{K}{4K''\sqrt{2N}} \sqrt{\frac{Ln_x \ln(1 + 1/\varepsilon') + \ln(3/\delta)}{2N}} \right\} \right) \leq \delta.$$

1327 Now we upper bound the summands in the square root to have

$$1328 \mathbb{P} \left(\text{GE}(\hat{\mathbf{H}}_N) > K \sqrt{\frac{\ln(3/\delta)}{2N}} + 4K'' \cdot \inf_{\varepsilon' \in (0, K/2K'']} \left\{ \varepsilon' + \frac{K}{4K''} \sqrt{\frac{Ln_x}{2N}} \sqrt{\ln(1 + 1/\varepsilon')} \right\} \right) \leq \delta.$$

1329 We upper bound the inf using the Proposition 2 to have

$$1330 \mathbb{P} \left(\text{GE}(\hat{\mathbf{H}}_N) > K \sqrt{\frac{\ln(3/\delta)}{2N}} + K \sqrt{\frac{2Ln_x \ln \left(1 + \max \left\{ \frac{4K''}{K} \sqrt{\frac{2N}{Ln_x}}, e-1 \right\} \right)}{N}} \right) \leq \delta.$$

1331 This concludes the proof.

1350 A.8 PROOFS OF COROLLARY 6
1351

1352 Authors of [Yang et al. \(2022\)](#) observed that GCN filter spectra are not only bounded but
1353 also sparse on real-world datasets like ZINC ([Irwin et al., 2012](#)), suggesting that Corol-
1354 lary 2 can be tightened. We now present generalization bounds for s -sparse spectra, i.e.,
1355 $\|\text{diag}^\dagger(\tilde{h}(\Lambda))\|_0 \leq s$.

1356 **Corollary 6.** *Let various symbols be as in Theorem 1 with $C_l = 1$. If \mathcal{FH} is bounded by
1357 1, and s -sparse, then w.p. of at least $1 - \delta$ we have*

$$1359 \text{GE}(\hat{\mathbf{H}}_N) \leq K \sqrt{\frac{2Ls}{N} \ln \left(1 + \max \left\{ \frac{4K''}{K} \sqrt{\frac{2N}{sL}}, e - 1 \right\} \right)} + K \sqrt{\frac{s \ln(en_x/s) + \ln(3/\delta)}{2N}}. \\ 1360 \quad (36) \\ 1361$$

1363 **Remarks.** The sample complexity is improved to $N \geq \mathcal{O}(Ls + s \ln(en_x/s) + \ln(1/\delta))$ in
1364 comparison to Corollary 2's $N \geq \mathcal{O}(Ln_x + \ln(1/\delta))$.
1365

1366 *Proof.* We use the classical result on the covering numbers for s -sparse vectors ([Chan-
1367 drasekaran et al., 2012](#)), the metric entropy satisfies $\ln(\mathcal{FH}, \|\cdot\|_2, \varepsilon) \leq \mathcal{O}(s \ln(1/\varepsilon) +
1368 s \ln(en_x/s))$. The rest follows as in Corollary 2. Now we state the metric entropy of the set
1369 of sparse vectors.

1370 **Lemma 8** (Metric entropy of sparse vectors). *The ε -metric entropy of the set of s -sparse
1371 vectors $\mathbb{B}_s = \{\theta \in \mathbb{R}^d : \|\theta\|_0 \leq s \cap \|\theta\|_2 \leq 1\}$ is given by*
1372

$$1373 \ln(\mathcal{N}(\mathbb{B}_s, \|\cdot\|_2, \varepsilon)) \leq s \ln(1 + 2/\varepsilon) + s \ln(en_x/s). \quad (37) \\ 1374$$

1375 *Proof.* For a fixed support $S \subseteq [d]$ of size s , the set of vectors is a s -dimensional ball in \mathbb{R}^s
1376 with radius 1. Lemma 7 gives us the upper bound $(1 + 2/\varepsilon)^s$. Since we do not know the
1377 support, we need to choose s coordinates from d and then cover the ball. The number of
1378 ways to choose s coordinates is $\binom{d}{s} \leq (ed/s)^s$. Therefore, the effective metric entropy is

$$1379 \ln(\mathcal{N}(\mathbb{B}_s, \|\cdot\|_2, \varepsilon)) \leq s \ln(1 + 2/\varepsilon) + s \ln(ed/s). \\ 1380$$

□

1381 **Proof of Corollary 6.** Following the proof technique of Corollary 2, define $K'' =
1382 \max\{K', K + 1\}$, we have

$$1383 \mathbb{P} \left(\text{GE}(\hat{\mathbf{H}}_N) > \inf_{\varepsilon \in (0, K]} \left\{ 2\varepsilon + K \sqrt{\frac{Ls \ln(1 + 2K''/\varepsilon) + Ls \ln(en_x/s) + \ln(3/\delta)}{2N}} \right\} \right) < \delta. \\ 1384$$

1385 Now we re-scale $\varepsilon = 2K''\varepsilon'$, this gives us

$$1386 \mathbb{P} \left(\text{GE}(\hat{\mathbf{H}}_N) > \inf_{\varepsilon' \in (0, K/2K'']} \left\{ 4K''\varepsilon' + K \sqrt{\frac{Ls \ln(1 + 1/\varepsilon') + Ls \ln(en_x/s) + \ln(3/\delta)}{2N}} \right\} \right) < \delta. \\ 1387$$

1388 By upper bounding the summands in the square root we have

$$1389 \mathbb{P} \left(\text{GE}(\hat{\mathbf{H}}_N) > K \sqrt{\frac{Ls \ln(en_x/s) + \ln(3/\delta)}{2N}} + \inf_{\varepsilon' \in (0, K/2K'']} \left\{ 4K''\varepsilon' + K \sqrt{\frac{Ls \ln(1 + 1/\varepsilon')}{2N}} \right\} \right) \\ 1390 < \delta. \\ 1391$$

1392 We take $4K''$ as common to have

$$1393 \mathbb{P} \left(\text{GE}(\hat{\mathbf{H}}_N) > K \sqrt{\frac{Ls \ln(en_x/s) + \ln(3/\delta)}{2N}} \right. \\ 1394 \left. + 4K'' \cdot \inf_{\varepsilon' \in (0, K/2K'']} \left\{ \varepsilon' + \frac{K}{4K''} \sqrt{\frac{Ls}{2N}} \sqrt{\ln(1 + 1/\varepsilon')} \right\} \right) < \delta. \\ 1395 \\ 1396$$

We upper bound the inf using Proposition 2 to have

$$\mathbb{P} \left(\text{GE}(\hat{\mathbf{H}}_N) > K \sqrt{\frac{Ls \ln(en_x/s) + \ln(3/\delta)}{2N}} + K \sqrt{\frac{2Ls}{N} \ln \left(1 + \max \left\{ \frac{4K''}{K} \sqrt{\frac{2N}{s}}, e - 1 \right\} \right)} \right) \\ < \delta.$$

This concludes the proof. \square

A.9 PROOFS OF COROLLARY 3

Next, we move onto the metric entropy of infinite-dimensional spaces. First, we consider the set of all Lipschitz functions on the d -dimensional unit ball \mathbb{B}^d .

Lemma 9 (Metric entropy of Lipschitz functions Wainwright (2019)). *Consider the class of Lipschitz functions*

$$\mathcal{F} := \{f : [0, 1]^d \rightarrow \mathbb{R} \mid f(0) = 0, \text{ and } \|f(\mathbf{x}) - f(\mathbf{x}')\|_2 \leq L\|\mathbf{x} - \mathbf{x}'\|_2 \quad \forall \mathbf{x}, \mathbf{x}' \in [0, 1]^d\}.$$

Then the ε -metric entropy of \mathcal{F} on the sup-norm $\|\cdot\|_\infty$ satisfies

$$\ln(\mathcal{N}(\mathcal{F}, \|\cdot\|_\infty, \varepsilon)) \leq \mathcal{O}((L/\varepsilon)^d). \quad (38)$$

Lemma 10. *Consider the set $\mathcal{A}(\{\lambda_j\}) := \{\{x_i\} : \forall i \in \mathbb{N}, f \in \mathcal{A}; x_i = h(\lambda_i)\}$, where $\mathcal{A} := \{f : \mathbb{C} \rightarrow \mathbb{C} : \forall \lambda, \lambda' \in \mathbb{C}, |f(\lambda) - f(\lambda')| \leq L|\lambda - \lambda'|, \|f\|_\infty \leq 1, f(0) = 0\}$. Then for any $\varepsilon > 0$ the metric entropy satisfies the inequality:*

$$\ln(\mathcal{N}(\mathcal{A}(\{\lambda_j\}), \|\cdot\|_2, \varepsilon)) \leq \mathcal{O}((L/\varepsilon)^4). \quad (39)$$

Proof. Consider two elements $\{x_i\}, \{x'_i\} \in \mathcal{A}(\{\lambda_j\})$, then we have $\|\{x_i\} - \{x'_i\}\|_\infty = \|\{h(\lambda_i)\} - \{h'(\lambda_i)\}\|_\infty$ for some $h, h' \in \mathcal{A}$. By definition we have that

$$\|\{x_i\} - \{x'_i\}\|_\infty = \|\{h(\lambda_i)\} - \{h'(\lambda_i)\}\|_\infty \leq \|h - h'\|_\infty. \quad (40)$$

For any arbitrary $\{x_i\} \in \mathcal{A}(\{\lambda_j\})$ generated by $h \in \mathcal{A}$, we can find a function $h' \in \mathcal{A}$ such that $\|h - h'\|_\infty \leq \varepsilon$ generating a sequence $\{h'(\lambda_i)\}$. Now clearly, ε -net of \mathcal{A} can generate a sequence that forms a ε -net of $\mathcal{A}(\{\lambda_j\})$.

Therefore, we have that $\ln(\mathcal{N}(\mathcal{A}(\{\lambda_j\}), \|\cdot\|_\infty, \varepsilon)) \leq \ln(\mathcal{N}(\mathcal{A}, \|\cdot\|_\infty, \varepsilon))$. We obtain the desired inequality by invoking result from Lemma 9 using the fact that $\mathbb{C} \cong \mathbb{R}^2$. \square

Next, we provide an auxiliary proposition that helps us compute the infimum in Theorem 1 for the scenario in Corollary 3.

Proposition 3. *Suppose $a, p > 0$ then the following holds true:*

$$\inf_{x>0} (x + ax^{-p}) < \left(p^{1/(1+p)} + p^{-p/(1+p)} \right) a^{1/(1+p)}. \quad (41)$$

Proof. We set the derivative of the objective to zero, i.e,

$$1 - apx^{-p-1} = 0 \Rightarrow x^* = (ap)^{1/(p+1)}.$$

Plugging this into the objective gives us the desired result. \square

Proof of Corollary 3. Now we instantiate Theorem 1 with $C_l = 1$, and metric entropy from Lemma 10. Then for some constant $C > 0$ we have

$$\mathbb{P} \left(\text{GE}(\hat{\mathbf{H}}_N) > \inf_{\varepsilon \in (0, K]} \left\{ 2\varepsilon + K \sqrt{\frac{CL(P/\varepsilon)^4 + \ln(3/\delta)}{2N}} \right\} \right) \leq \delta,$$

where $K'' = \max\{K', K + 1\}$. We re-scale $\varepsilon = P\varepsilon'/C^{1/4}$, this gives us

$$\mathbb{P} \left(\text{GE}(\hat{\mathbf{H}}_N) > \inf_{\varepsilon' \in (0, KC^{1/4}/P]} \left\{ \frac{2P}{C^{1/4}} \varepsilon' + K \sqrt{\frac{L/\varepsilon'^4 + \ln(3/\delta)}{2N}} \right\} \right) \leq \delta.$$

1458 Now we upper bound the summands in the square root to have
1459

$$1460 \mathbb{P} \left(\text{GE}(\hat{\mathbf{H}}_N) > K \sqrt{\frac{\ln(3/\delta)}{2N}} + \frac{2P}{C^{1/4}} \cdot \inf_{\varepsilon' \in (0, KC^{1/4}/P]} \left\{ \varepsilon' + \frac{KC^{1/4}}{P\sqrt{8N/L}} \varepsilon'^{-2} \right\} \right) \leq \delta.$$

1463 From the Proposition 2 with $p = 2$, we have
1464

$$1465 \mathbb{P} \left(\text{GE}(\hat{\mathbf{H}}_N) > K \sqrt{\frac{\ln(3/\delta)}{2N}} + \frac{2P}{C^{1/4}} \left(2^{1/3} + 2^{-2/3} \right) \left(\frac{KC^{1/4}}{P\sqrt{8N/L}} \right)^{1/3} \right) \leq \delta.$$

1468 Simplifying the constants gives us the desired result.
1469

1470 PROOFS OF COROLLARY 4

1472 **Lemma 11.** Consider the set of countably infinite dimensional vector whose entries poly-
1473 nomially decay as C/i^α , i.e., $\mathcal{A} := \{\{x_i\} \in (\mathbb{R}) : \forall i \in \mathbb{N}; |x_i| \leq \frac{C}{i^\alpha}\}$. If $\alpha > 1/2$, then for
1474 any $\varepsilon > 0$ the metric entropy satisfies the inequality:

$$1475 \ln(\mathcal{N}(\mathcal{A}, \|\cdot\|_2, \varepsilon)) \leq \left(\frac{16C^2}{2\alpha-1} \right)^{1/(2\alpha-1)} \varepsilon^{-2/(2\alpha-1)} \ln \left(1 + \frac{4C\sqrt{\zeta(2\alpha)}}{\varepsilon} \right), \quad (42)$$

1478 where $\zeta(\cdot)$ is the Riemann zeta function.
1479

1480 *Proof.* We will construct a sub-set defined as
1481

$$1482 \mathcal{A}_d := \left\{ \{y_i\} \in (\mathbb{R}) : \forall i \in [d], |y_i| \leq \frac{C}{i^\alpha} \text{ and } \forall j > d, y_j = 0 \right\}. \quad (43)$$

1485 For any element $\{x_i\}, \{x'_i\} \in \mathcal{A}, \{y_i\} \in \mathcal{A}_d$ and $\{y'_i\} \in \mathcal{C}(\mathcal{A}_d, \varepsilon/2)$ we have the inequality
1486

$$1487 \|\{x_i\} - \{x'_i\}\|_2 \leq \|\{x_i\} - \{y_i\}\|_2 + \|\{y'_i\} - \{x'_i\}\|_2 + \|\{y_i\} - \{y'_i\}\|_2. \quad (44)$$

1488 Using the fact that $\{y'_i\} \in \mathcal{C}(\mathcal{A}_d, \varepsilon/2)$ we have
1489

$$1490 \|\{x_i\} - \{x'_i\}\|_2 \leq \varepsilon/2 + \|\{x_i\} - \{y_i\}\|_2 + \|\{y'_i\} - \{x'_i\}\|_2, \quad (45)$$

1491 we now apply the triangular inequality to obtain,
1492

$$1493 \|\{x_i\} - \{x'_i\}\|_2 \leq \varepsilon/2 + 2 \sqrt{\sum_{j>d} \left(\frac{C}{j^\alpha} \right)^2} \leq \frac{\varepsilon}{2} + \frac{2C}{\sqrt{2\alpha-1}} d^{-(2\alpha-1)/2}. \quad (46)$$

1496 Now choose d such that $\frac{2C}{\sqrt{2\alpha-1}} d^{-(2\alpha-1)/2} \leq \varepsilon/2$. This requires that
1497

$$1498 d \geq d(\varepsilon) := \left(\frac{4C}{\sqrt{2\alpha-1}} \varepsilon^{-1} \right)^{2/(2\alpha-1)}.$$

1501 When $d \geq d(\varepsilon)$ we have that $\|\{x_i\} - \{x'_i\}\|_2 \leq \varepsilon$. By definition the metric entropy of \mathcal{A} is
1502 smaller than the metric entropy of $\mathcal{A}_d(\varepsilon)$. Then
1503

$$1504 \ln(\mathcal{N}(\mathcal{A}, \|\cdot\|_2, \varepsilon)) \leq \ln(\mathcal{N}(\mathcal{A}_{d(\varepsilon)}, \|\cdot\|_2, \varepsilon/2)) \leq d(\varepsilon) \ln \left(1 + \frac{4}{\varepsilon} \sqrt{\left(\sum_{i>0} C^2/i^{2\alpha} \right)} \right). \quad (47)$$

1507 On simplification we have
1508

$$1509 \ln(\mathcal{N}(\mathcal{A}, \|\cdot\|_2, \varepsilon)) \leq \left(\frac{16C^2}{2\alpha-1} \right)^{1/(2\alpha-1)} \varepsilon^{-2/(2\alpha-1)} \ln \left(1 + \frac{4C\sqrt{\zeta(2\alpha)}}{\varepsilon} \right). \quad (48)$$

1511 This gives us the desired result. \square

1512 **Corollary 7.** Consider the set of countably infinite dimensional vector whose entries polynomially decay as C/i^α , i.e., $\mathcal{A} := \{\{x_i\} \in (\mathbb{C}) : \forall i \in \mathbb{N}; |x_i| \leq \frac{C}{i^\alpha}\}$. If $\alpha > 1/2$, then for any $\varepsilon > 0$ the metric entropy satisfies the inequality:

$$1516 \quad \ln(\mathcal{N}(\mathcal{A}, \|\cdot\|_2, \varepsilon)) \leq 2 \left(\frac{16C^2}{2\alpha-1} \right)^{1/(2\alpha-1)} \varepsilon^{-2/(2\alpha-1)} \ln \left(1 + \frac{4C\sqrt{\zeta(2\alpha)}}{\varepsilon} \right), \quad (49)$$

1518 where $\zeta(\cdot)$ is the Riemann zeta function.

1520 *Proof.* The proof is same as Lemma 11, except that the metric entropy of $\mathcal{A}_{d(\varepsilon)}$ is upper
1521 bounded by $2d(\varepsilon) \ln \left(1 + \frac{4}{\varepsilon} \sqrt{(\sum_{i>0} C^2/i^{2\alpha})} \right)$. \square

1524 **Proposition 4.** Suppose $a, p > 0$ then the following holds true:

$$1525 \quad \inf_{x>0} \left(x + a\sqrt{x^{-2p} \ln(1+1/x)} \right) < 2(ap)^{1/(p+1)} \sqrt{\ln(1 + \max\{(ap)^{-1/(1+p)}, e^{p^2} - 1\})}. \quad (50)$$

1528 *Proof.* Choose $x = (ap)^{1/(p+1)}$ as the candidate point to upper bound the infimum. Then
1529 we have

$$1530 \quad \inf_{x>0} \left(x + a\sqrt{x^{-2p} \ln(1+1/x)} \right) < (ap)^{1/(p+1)} + a\sqrt{(ap)^{-2p/(p+1)} \ln(1 + (ap)^{-1/(p+1)})}.$$

1532 Taking $(ap)^{1/(p+1)}$ out common we have

$$1534 \quad \inf_{x>0} \left(x + a\sqrt{x^{-2p} \ln(1+1/x)} \right) < (ap)^{1/(p+1)} \left(p + \sqrt{\ln(1 + (ap)^{-1/(p+1)})} \right).$$

1536 By applying Cauchy-Schwarz inequality we have the desired result. \square

1538 **Proof of Corollary 4.** From Theorem 1 and Corollary 7 we have

$$1540 \quad \mathbb{P} \left(\text{GE}(\hat{\mathbf{H}}_N) > \inf_{\varepsilon \in (0, K]} \left\{ 2\varepsilon + K \sqrt{\frac{w_1 L \varepsilon^{-2/(2k-1)} \ln(1 + w_2/\varepsilon) + \ln(3/\delta)}{2N}} \right\} \right) < \delta,$$

1543 where $w_1 = 2 \left(\frac{16A_{\text{pass}}^2}{2k-1} \right)^{1/(2k-1)}$, and $w_2 = 4A_{\text{pass}}\sqrt{\zeta(2k)} \cdot \max\{K', K + 1\}$.

1545 Now re-scale $\varepsilon = w_2\varepsilon'$, this gives us

$$1547 \quad \mathbb{P} \left(\text{GE}(\hat{\mathbf{H}}_N) > \inf_{\varepsilon' \in (0, K/w_2]} \left\{ 2w_2\varepsilon' + K \sqrt{\frac{w_1 w_2^{-2/(2k-1)} L \varepsilon'^{-2/(2k-1)} \ln(1 + 1/\varepsilon') + \ln(3/\delta)}{2N}} \right\} \right) \\ 1548 \quad \leq \delta.$$

1551 Now we upper bound the summands in the square root to have

$$1553 \quad \mathbb{P} \left(\text{GE}(\hat{\mathbf{H}}_N) > K \sqrt{\frac{\ln(3/\delta)}{2N}} \right. \\ 1554 \quad \left. + 2w_2 \cdot \inf_{\varepsilon' \in (0, K/w_2]} \left\{ \varepsilon' + \frac{K}{2w_2^{2k/(2k-1)}} \sqrt{\frac{w_1 L}{2N}} \sqrt{\varepsilon'^{-2/(2k-1)} \ln(1 + 1/\varepsilon')} \right\} \right) \leq \delta.$$

1558 From Proposition 4 with $p = 1/(2k-1)$, we have

$$1559 \quad \mathbb{P} \left(\text{GE}(\hat{\mathbf{H}}_N) > K \sqrt{\frac{\ln(3/\delta)}{2N}} + 4 \left(\frac{K}{2(2k-1)} \sqrt{\frac{w_1 L}{2}} \right)^{(2k-1)/(2k)} N^{-(2k-1)/4k} \right. \\ 1560 \quad \left. \times \sqrt{\ln \left(1 + \max \left\{ w_2 \left(\frac{2(2k-1)}{K} \sqrt{\frac{2}{w_1 L}} \right)^{1-1/2k} N^{(2k-1)/4k}, e^{1/(2k-1)^2} - 1 \right\} \right)} \right) \\ 1562 \quad \leq \delta.$$

1566 Now let us apply the limit $k \rightarrow \infty$, the term $\lim_{k \rightarrow \infty} N^{(2k-1)/4k} \rightarrow \sqrt{N}$, $\lim_{k \rightarrow \infty} e^{1/(2k-1)^2} -$
 1567 $1 \rightarrow 0$. $\lim_{k \rightarrow \infty} w_2 \rightarrow 4A_{\text{pass}}$ because $\lim_{k \rightarrow \infty} \zeta(2k) \rightarrow 1$. Finally we have the coefficient
 1568 term

$$\begin{aligned}
 1569 \lim_{k \rightarrow \infty} \left(\frac{K}{2(2k-1)} \sqrt{\frac{w_1 L}{2}} \right)^{(2k-1)/(2k)} &= \lim_{k \rightarrow \infty} \left(\frac{K}{2(2k-1)\sqrt{2}} \right)^{(2k-1)/(2k)} (Lw_1)^{(2k-1)/4k} \\
 1570 &= \lim_{k' \rightarrow \infty} \left(\frac{K}{2\sqrt{2}k'} \right)^{1/(k'+1)} \\
 1571 &\quad \times \lim_{k \rightarrow \infty} (2L)^{(2k-1)/4k} \left(\frac{16A_{\text{pass}}^2}{2k-1} \right)^{1/4k} \rightarrow \sqrt{2L}.
 \end{aligned}$$

1572 Thus when $k \rightarrow \infty$ we have

$$1573 \mathbb{P} \left(\text{GE}(\hat{\mathbf{H}}_N) > K \sqrt{\frac{\ln(3/\delta)}{2N}} + 8 \sqrt{\frac{L \ln(1 + A_{\text{pass}} \sqrt{8N/L})}{2N}} \right) \leq \delta$$

1574 This concludes the proof.

1575
 1576
 1577
 1578
 1579
 1580
 1581
 1582
 1583
 1584
 1585
 1586
 1587
 1588
 1589
 1590
 1591
 1592
 1593
 1594
 1595
 1596
 1597
 1598
 1599
 1600
 1601
 1602
 1603
 1604
 1605
 1606
 1607
 1608
 1609
 1610
 1611
 1612
 1613
 1614
 1615
 1616
 1617
 1618
 1619